DETECTION OF LUNG NODULES AND CLASSIFICATION USING DEEP LEARNING NETWORK

By

SALMAN AHMED

NATIONAL UNIVERSITY OF MODERN LANGUAGES

ISLAMABAD

August, 2022

Detection of Lung Nodules and Classification Using Deep Learning Network

By

SALMAN AHMED

MSCS, National University of Modern Languages, Islamabad, 2022

A THESIS SUBMITTED IN PARTIAL FULFILLMENT OF THE REQUIREMENT FOR THE DEGREE OF

MASTERS OF SCIENCE

In **Computer Science**

To

FACULTY OF ENGINEERING & COMPUTER SCIENCE

NATIONAL UNIVERSITY OF MODERN LANGUAGES ISLAMABAD

PLAGIARISM UNDERTAKING

I take full responsibility of the research work conducted during the Masters Thesis titled *Detection of Lung Nodules and Classification using Deep Learning Network*. I solemnly declare that the research work presented in the thesis is done solely by me with no significant help from any other person; however, small help wherever taken is duly acknowledged. I have also written the complete thesis by myself. Moreover, I have not presented this thesis (or substantially similar research work) or any part of the thesis previously to any other degree awarding institution within Pakistan or abroad.

I understand that the management of the National University of Modern Languages has a zero-tolerance policy toward plagiarism. Therefore, I as an author of the above-mentioned thesis, solemnly declare that no portion of my thesis has been plagiarized and any material used in the thesis from other sources is properly referenced. Moreover, the thesis does not contain any literal citing of more than 70 words (total) even by giving a reference unless I have the written permission of the publisher to do so. Furthermore, the work presented in the thesis is my own original work and I have positively cited the related work of the other researchers by clearly differentiating my work from their relevant work.

I further understand that if I am found guilty of any form of plagiarism in my thesis work even after my graduation, the University reserves the right to revoke my Masters degree. Moreover, the University will also have the right to publish my name on its website that keeps a record of the students who plagiarized in their thesis work.

_____
Signature of Candidate

Salman Ahmed
Name of Candidate

31 August 2022
Date

THESIS AND DEFENSE APPROVAL FORM

The undersigned certify that they have read the following thesis, examined the defense, are satisfied with overall exam performance, and recommend the thesis to the Faculty of Engineering and Computer Sciences for acceptance.

Thesis Title: Detection of Lung Nodules and Classification Using Deep Learning Network

Submitted By: Salman Ahmed **Registration #:** 46 MS/CS/F20

Master of Science in Computer Science (MSCS)
Title of the Degree

Computer Science
Name of Discipline

Dr. Fazli Subhan _____
Name of Research Supervisor Signature of Research Supervisor

Dr. Basit Shahzad _____
Name of Dean (FE&CS) Signature of Dean (FE&CS)

Prof. Dr. Muhammad Safeer Awan _____
Name of Pro-Rector Academics Signature of Pro-Rector Academics

31 August , 2022

AUTHOR'S DECLARATION

I Salman Ahmed S/O Noor ul Hijab, hereby state that my Masters thesis titled *Detection of Lungs Nodules and Classification Using Deep Learning Network* is my own work and it has not been previously submitted by me for taking partial or full credit for the award of any degree at this University or anywhere else in the world. If my statement is found to be incorrect, at any time even after my graduation, the University has the right to revoke my Masters degree.

Signature of Candidate

Salman Ahmed
Name of Candidate

31 August 2022
Date

ABSTRACT

One of the leading causes of cancer-related deaths around the world is lung cancer. The presence of lung nodules helps to detect lung cancer. Lung nodules are mostly small, rounded, spherical-shaped masses of vessels or tissues in the lung region. Accurate detection and classification of pulmonary nodules present in the computer tomography (CT) scan images are one of the major and complex problems. These lung nodules vary in size and shape and most of the time they are interlinked. Due to their size and location, it is difficult to detect them through naked eyes in the CT scan images. To address this problem, many researchers have used machine learning and computer vision-based techniques but these studies mostly do not consider the small size of lung nodules and ignore them. Moreover, these studies also suffer from the false-positive ratio which greatly affects the accuracy of the system. In this study, I have developed a deep learning network model VGG16 for accurate detection and classification of pulmonary nodules by considering all sizes of nodules from small sizes to large ones. Furthermore, the false-positive ratio is also improved by using unbiased data. VGG16 model stands at number one in terms of detection and it was unbeatable to date. This technique involved the steps of lung nodules image data acquisition, preprocessing of the images, data augmentation, and feature extraction using a deep convolutional neural network. After that, the deep CNN model is trained and classification of pulmonary nodules into cancerous and non-cancerous has been performed. This research work is tested and evaluated on LIDC-IDRI openly available dataset. The experimental work shows that the DCNN model VGG 16 achieved better performance with an accuracy of 93.55%, recall of 93.54%, and precision of 87.15% respectively which is better than the results gained by a previous study in this domain 91.60%.

Keywords—Lung Nodules, Lung Cancer, Deep Learning, VGG 16, Lung Nodules detection, Lung Nodules Classification

TABLE OF CONTENTS

LIST OF TABLES

LIST OF FIGURES

LIST OF ABBREVIATIONS

ACS	-	American Cancer Society
SCLC	-	Small Cell Lung Cancer
ML	-	Machine Learning
DL	-	Deep Learning
NSCLC	-	Non-Small Cell Cancer
CT	-	Computed Tomography
VGG	-	Visual Geometry Group
DICOM	-	Digital Imaging and Communications in Medicine
CAD	-	Computer Aided Detection

ACKNOWLEDGMENT

First of all, I would like to thank Almighty ALLAH (S.W.T), the Merciful and the Beneficent, who blessed me with good health and skills to achieve this goal. I would like to record my gratitude to my worthy supervisor Dr. Fazli Subhan for his guidance, advice, and supervision to do this research work. I would also like to thank all those people who made this possible, especially my parents, brothers, all family members, and friends. I am also thankful to all my teachers in the university who are imparting knowledge, sharing their expertise related to different domains, and doing a noble and grateful job of teaching, a profession of our Holy Prophet Hazrat MUHAMMAD (P.B.U.H)

I shall also acknowledge the extended assistance from the administration of the Department of Computer Sciences who supported me all through my research experience and simplified the challenges I faced. For all whom I did not mention but I shall not neglect their significant contribution, thanks for everything.

DEDICATION

This thesis work is dedicated to my parents, brothers, my beloved niece Aabroo Gul, my teachers, all family members, and friend

CHAPTER 1

INTRODUCTION

1.1 Overview

In this chapter, the background, and introduction to lung cancer have been discussed. Moreover, facts and figures related to lung cancer around the world are also part of this chapter supported by credible sources and references. Reasons and causes of lung cancer are also part of this discussion. There are various sizes of lung cancer nodules that have been explained with the support of relevant figures. All those problems associated with the detection and classification of lungs nodules which have been addressed in the previous studies using different techniques including machine learning, computer vision, and deep learning are also part of the discussion and those problems which have been ignored in these studies have also been identified and are the main focus of this research work. After that, the motivation to carry out this research work, main problem statement, research questions that are the base of this research work and the possible research objectives that are the main goal to achieve in this research work, Scope of the work and the contribution of this research work has been discussed.

1.2 Introduction

Cancer is a disease that shows up in a variety of forms and it's commonly associated with abnormal cell groups. These abnormal cells cause the uncontrolled growth and division of cells to produce tumors [1]. In 2020, a report released by the World Health Organization (WHO) that cancer is the most common cause of death around the world, with approximately 10 million people deaths in 2020, accounting for one in every six deaths [2]. Lung cancer produces in vessels or tissues of the lung, particularly within the same cells that line the air passages. Available statistics show that lung cancer is the 2nd most common cause of cancer-related death globally. Around 2.21

million cases were reported at a ratio of 11.4 % and more than 1.8 million lung cancer deaths occurred at a ratio of 18% in the year 2020 [3]. It is most common in men as compared to women around the world. Some of the major reasons for lung cancer is consuming arsenic-containing drinking water. While, consumption of alcohol, smoke toxic particles, outdoor air pollution, and red meat are also one of the leading causes of lung cancers. According to the 2022 lung cancer report published by the American Cancer Society, the estimated number of new lung cases and deaths in the USA are 236,740 and 130,180 respectively[4]. Figure 1.1 shows the total number of new lung cases and deaths in the USA during the last five years (2018-2022). Lung cancer has two types, small-cell lung cancer (SCLC) and non-small cell lung cancer (NSCLC). Lung cancer that occurs and spreads slowly is called NSCLC. Pulmonary cancer that occurs and spreads quickly is called SCLS. Around 80 to 85 percent of pulmonary cancer cases are NSCLC and the remaining 10 to 15 % of lung cancer cases are SCLC [5].

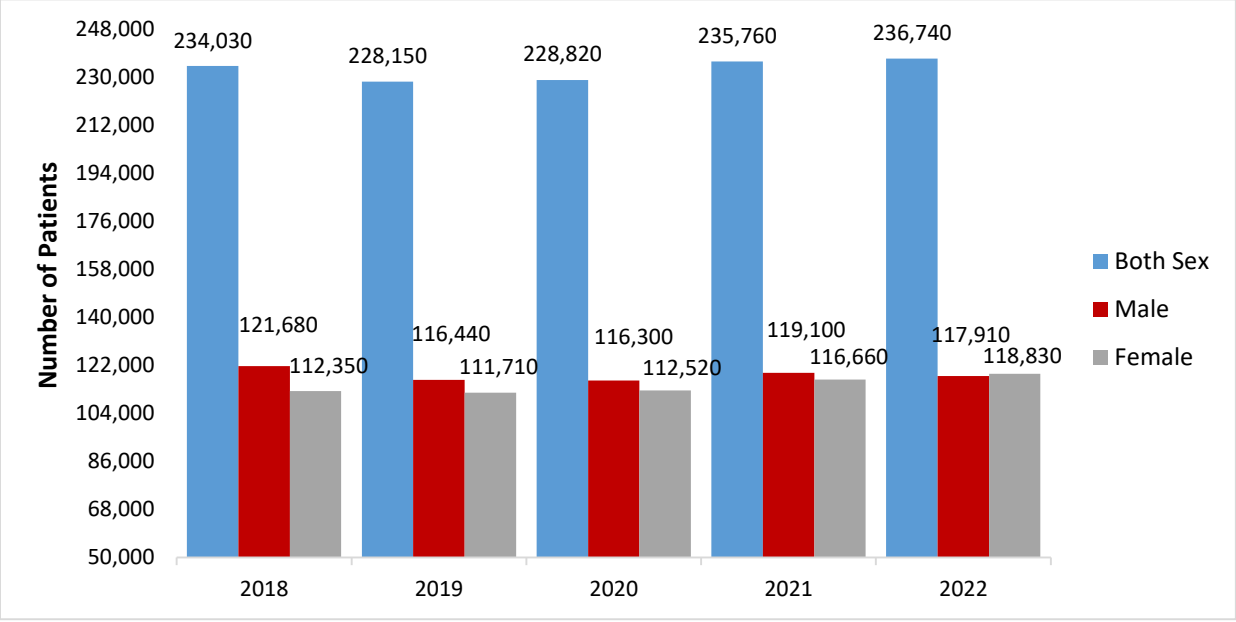

(A)

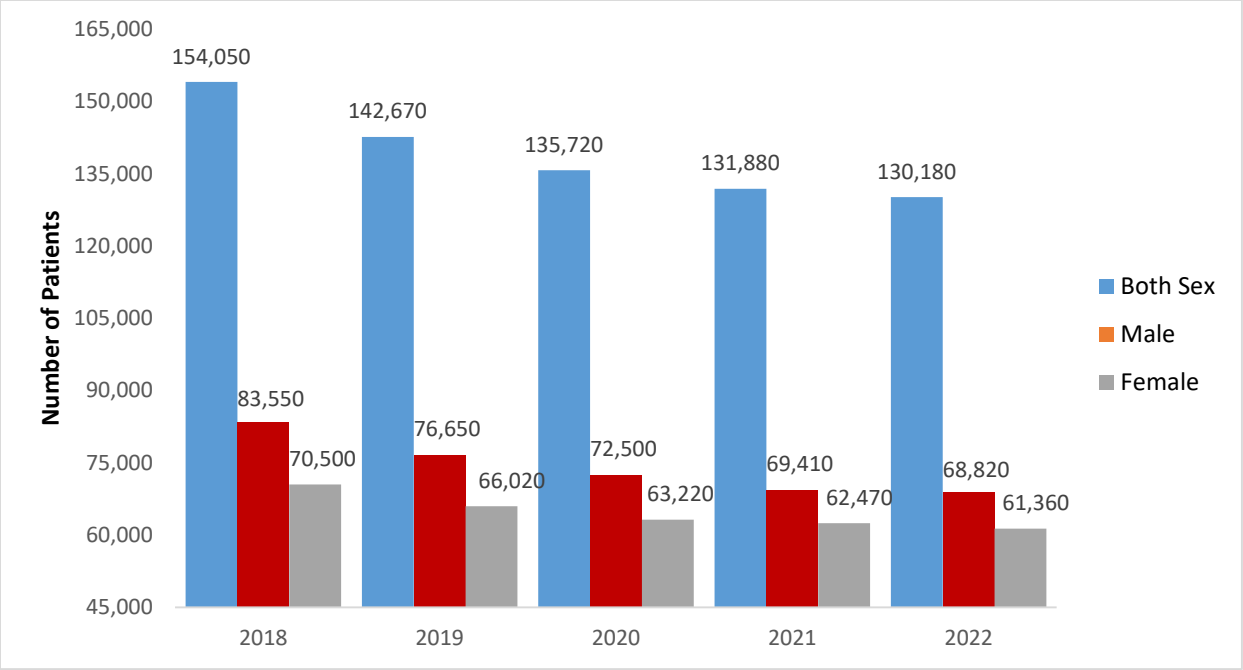

(B)

Figure 1.1: American Cancer Society – ACS [4] from 2018–2022 show a lung cancer data in the United State. (**A**) Numbers of estimated new lung cancer patients. (**B**) Numbers of estimated lung cancer expire patients.

In developing countries, about 70 percent of patients are diagnosed with lung cancer at advanced stages without effective or proper cures. The five-year survival rate for advanced stage of lung cancer in China is about 16% [6]. However, the 5-year rate of survival can reach 70% if lung cancer is detected and diagnosed at an early phase [7]. Lung nodules help to identify lung cancers while detecting these lung nodules is one of the difficult tasks due to their location, shape, and size. Detection of the lung nodules at an early stage can help to prevent and timely treatment of lung cancer but it is one of the difficult tasks. These lung nodules can be as small as less than 3mm size while can be large than this. Nodules with diameters < 3mm are known as micro-nodules. In terms of location, pulmonary nodules are defined into 4 classes (well-circumscribed, Juxta-vasculature, Pleural tail and Juxta-pleural). Well-circumscribed: positioned in the middle of the lung with no connections to the vasculature. Juxta-vascular: has a connection to the vessels and even placed in the middle of the lung. Pleural tail: is located on the pleural surface and linked by a thin structure. Juxta-pleural: strongly attached to Pleural Surface [8]. Furthermore, lung nodules

are divided into solid nodules (SNs) and sub-solid nodules (SSNs) on the basis of internal texture. SSNs are further sub-divided into pure ground-glass nodules (GGN) and as well as into part-solid types nodules. SNs: suppress underlying functioning tissues of the lungs. Sub-solid lung nodules have limited and partial ground-glass opacity (GGO). These lesions have higher density opacifications than the surrounding tissues and do not hide underlying Broncho vascular structure [9]. Figure 1.2 shows a sample image of different nodules types. Sometimes, small candidate nodules are ignored in the detection process due to their small size and clinicians with naked eyes can miss them to identify in the computed tomography (CT) scan images. For this purpose, different computer-aided diagnosis (CAD) systems have been developed by many researchers to address this problem using different technologies including computer vision, machine learning (ML) and deep learning (DL).

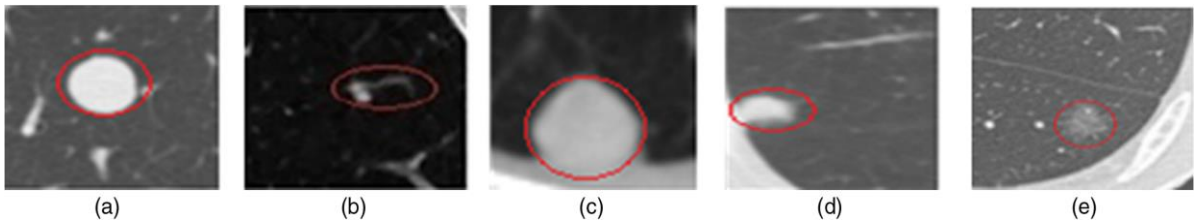

Figure 1.2: show different samples of pulmonary nodule types. (a) Well-circumscribed /solid, (b) juxtavascular /subsolid, (c) juxtapleural, (d) pleural-tail, (e) GGO nodule [10]

These systems have been designed and developed for different purpose including nodule segmentation, localization, detection of candidate nodules, false positive reduction and classification. Most of the systems have worked on just one perspective detection localization or classification, while some have worked on all of these either on segmentation, detection and localization or detection and classification. CT scan-based publically image datasets have been used with varying features in most of the studies while some researchers have worked on this problem using their own dataset collected through a process over a period of time. Most of the work in this domain is related to lung nodules detections. These nodules are classified into benign and malignant. Benign nodules usually not spread to other lung region parts as these are considered

non-cancerous while malignant nodules are considered cancerous ones and usually spread to other parts of the lungs as well. Lung nodules present in a CT scan image are shown below in figure 1.3.

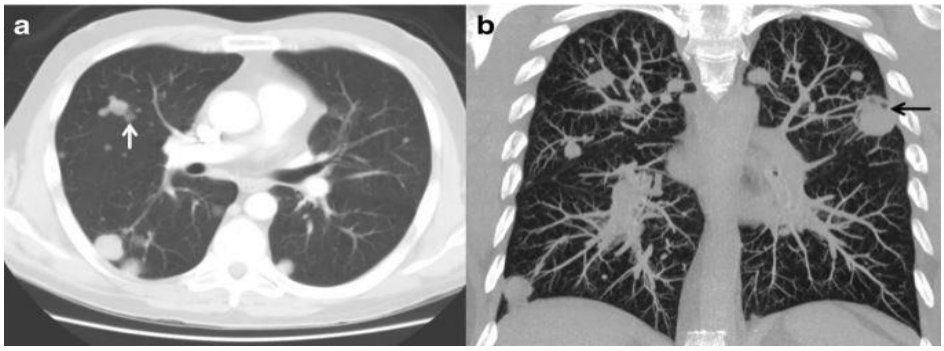

Figure 1.3: Lung nodules present in a CT scan image

Deep learning, machine learning and computer vision techniques have been used by different researchers in this domain till date. Both Computer vision and ML techniques work better on the small size of the dataset but can face difficulty with data of large size and diversity. Many machine learning models have been used and still are being used due to their effectiveness against small datasets[11]. For large size of the database, DL techniques [12] have been effective while deep learning models struggle with a small size of the dataset. Deep learning models have been mostly in use for the last 5 years as the introduction of the high computational power of processors. Before that, machine learning models were mostly being used as deep learning models require high computational resources. But the trend of using deep neural network models in various fields is gaining upward direction due to the availability of high processing computational resources. Deep learning models have been found useful to detect and classify pulmonary candidate nodules which can play a major role in the early and correct detection of pulmonary nodules. As these lung nodules help to diagnose whether a patient has lung cancer or not. So, detection and classification of each and every lung nodule are very important.

1.3 Motivation

The motivation behind working on this research is to help those people who are suffering from lung cancer or can develop lung cancer so that exact stage-wise detection can be done on an early basis. This research will also be helpful for the doctors in timely and accurate detection of the lung nodules. Detection and diagnosis of lung cancer without a CAD system is a very difficult task. Small lung nodules can be ignored by the doctors during the diagnosis process by seeing the CT scan images from the naked eye. So, this unintentional negligence can be very dangerous. Moreover, some computer-aided and proposed systems do not consider the small size of nodules which can give biased results. There are some systems and proposed methodologies that struggle to gain good accuracy. In this study, [13] developed a new approach to segment lung volume using CT scan images. And they applied the SVM model based on hybrid features. For this purpose a small size of lung nodule dataset was used and ignoring the data augmentation technique. In nodule classification stage, FPs score was not informed. In another research, [14] authors analyzed and implemented five different algorithms with optimized performance to extract cancer from the lung images including guaranteed convergence particle swarm optimization, k-median clustering, inertia-weighted PSO, k-means clustering, and particle swarm optimization. Here only 20 lung images samples have been used for the validation purpose. In this study [15] author used segmentation technique based morphological operation, effectively remove the trachea's influence inside lung nodule images. They used ROI extraction based circular filter, to reduce the no. of false nodules and improved the performance speed. Here the cost of system was reduced but still need work to improve its accuracy. So, it needs time to consider all the factors and features that can play an essential role in the detection and classification of lung nodules so that early-stage accurate detection and treatment can be started for lungs cancer. And such a system should be cost-effective and trustable.

1.4 Problem Statements

Detection and accurate classification of lung nodules is a very challenging task due to its complex nature. Lung nodules location, size, and shapes make it difficult to detect and classify.

Many systems have been proposed to address the detection and classification problem but the selective nature of characteristics and ignoring the small details raise questions on their validity. Moreover, computer vision and machine learning models just only work on the small size of datasets and do not perform well on large size datasets and complex classification tasks. While previous deep learning methods have limitations in terms of improving the detection performance on the small size of nodules and ground nodules which were mostly ignored in their study and the accuracy of the results due to the false-positive ratio. To address these problems, we will use all relevant features and small size nodules in this study so that accurate and correct classification can be done using deep learning-based techniques.

1.5 Research Questions

Research work is always carried out based on some research questions which are basically related to the limitations present in the previous research studies. Research questions based on which this research study is being carried out are given below.

RQ-1: How improved and accurate CAD system for detection and classification will be carried out?

RQ-2: How false-positive ratio will be reduced and accuracy will be improved?

RQ-3: How different shape of small size nodules consideration will help to gain accurate detection and classification?

1.6 Research Objectives

The main objective of this research work is to develop such a framework using deep learning technologies which can help to detect and classify the lung nodules so that timely and accurate treatment can be started. The objectives of this research work are given below.

- Improved and accurate detection and classification using DDN based VGG16 model
- To improve the accuracy and to reduce the false-positive ratio, the dataset will be preprocessed and augmented to remove the noise, outliers and unbiased the sample
- Lung nodules of all sizes will be considered here which will play a significant role in the accurate detection and classification.

1.7 Contribution and Signification

In this research work, our contribution is that we are considering here small nodules along with relatively large size of nodules for better and accurate detection and classification. Moreover, we are also eyeing to improve the accuracy by decreasing the false positive rate that has been found in previous studies. Reducing the false-positive ratio will increase the accuracy of the system.

1.8 Scope of the Study

As this study is related to the accurate detection and classification of lung nodules so it will be helpful to detect lungs cancer at an early stage using deep learning techniques. This proposed system will help doctors in the timely and accurate detection of lung nodules so that they can take decisions regarding the treatment of the patient at an early stage. So, this study can be used in the medical domain to help the professionals just like other computer-aided diagnostic systems which are being used successfully in heart-related diseases, skin cancers and brain tumor detections.

1.9 Thesis Organization

This research work has been organized in terms of different chapters. In 1st chapter, introduction is given in which introduction of the topic, background, motivation, problem

statement, research questions, research objectives, scope of the research study and the main contribution and signification of this research work has been discussed. While in 2nd chapter, literature review of the most relevant research work has been discussed with their major contributions and limitations and also a table of comparative study is also given in this chapter, while at the end of the chapter, summary of the chapter is given. In 3rd chapter, proposed methodology have been discussed in detail including the techniques and models that have been used to implement this research work using Python programming language. Here, architecture of the deep learning model and the dataset have been discussed in detail as well. In 4th chapter, experimental setup of the research work has been discussed. In 5th chapter, results of the research work and the hyperparameters that have been used in this research work have been discussed and the comparison of results with previous relevant studies have been given. While 6th chapter is the last chapter of this study in which, conclusion of the research work with possible future direction in this field has been discussed.

CHAPTER 2

LITERATURE REVIEW

2.1 Overview

This chapter presents the literature review of the most recent and relevant studies that have been carried out by different researchers in this domain using different techniques and datasets. In this chapter, research studies that have been carried out in the fields of machine learning, deep learning and computer vision are discussed. Literature review have been carried out by focusing on the problems that have been identified by the researchers and addressed, size and characteristics of the datasets that have been used in various studies, authenticity of the research work and the results by examining different parameters and the limitations of these studies. Moreover, a table of comparative studies is also given in this chapter which depicts the domains, techniques, and limitations of these studies.

2.2 Literature Review

Changmiao wanga et al., [16] developed a lung nodules detection system and addressed the problem of a higher false-positive ratio. Here, the authors reduced the false-positive ratio using the fusion of hand-crafted and deep features of training data. The authors carried out this study based on three modules including preprocessing of the dataset, suppression of the ribs, and segmentation of the lung nodules. Here, a publically available dataset JSRT is used for validation purposes. Using deep fusion features resulted in a false-positive ratio of 1.19 on a single image and achieved the specificity and sensitivity of 96.2% and 69.3% respectively. While false-positive

ratio achieved on a single image using hand-crafted features is 1.45 and resulted in specificity and sensitivity of 95.4% and 62% respectively.

Nima Tajbaksh and Kenji Suzuki [17] in this study carried out a machine learning models comparison of two classes that have been used in the medical images analysis. As handcrafted features take too much time which can be decreased using learning machines that map the raw input data directly to the required output. There are two classes of end-to-end learning machines including convolutional neural networks (CNNs) and massive training artificial neural networks (MTANNs). These both are being used in medical images analysis tasks but convolutional neural networks have been popular for the past few years. To compare these two learning machines, the authors here considered the two topics of medical image analysis including the difference between cancerous and non-cancerous lung nodules and the detection of candidate nodules from the computed tomographic images. For better comparison, the authors evaluated the performance of these learning machines considering 4 CNNs and 2 MTANNs. Results show that MTANSS achieved better performance as compared to CNN. The false-positive ratio generated by CNN's is 22.7 for a single patient with a sensitivity of 100% while MTANNs achieved the same sensitivity score but generated the false-positive ratio for a single patient as 2.7. Results achieved by MTANNs and CNNs in terms of AUC are 88.06% and 77.55% respectively.

Huang et al., [18] worked on the detection of candidate lung nodules using computed tomography (CT) low dose images. For this purpose, the authors proposed a convolutional neural network-based 3D architecture for the detection of lung nodules. Structural anatomy and a-priori knowledge of lung nodules have been considered in this system. Nodule candidates have been generated here using a filter based on the local geometric model. To differentiate the non-nodules and nodules from the input images, a 3D CNN model has been trained using the 3D cubes of candidate nodules. A Dataset of 99 computed tomography scan images have been used and to increase the number of images, a data augmentation technique has been used here. Promising and state-of-the-art results achieved by this system are better than 2D-based CNN models.

In this paper, Ding et al., [19] addressed the accurate detection of lung nodules by proposing a novel system using deep convolutional neural networks from the CT images. For the

detection of candidates from the axial slices, a faster R-CNN is used here by the authors. While to reduce the false-positive ratio, a 3D DCNN has been used. To validate the proposed system, the LUNA16 challenge data set has been used which resulted in an FROC score of 0.891 placing the proposed architecture in 1st position on the leader board of this challenge.

One of the challenging tasks in the lung nodules detection systems is the decrease of the false-positive ratio as it is important in the lung nodules detection process. To address this issue, Dou et al., [20] proposed a novel approach based on 3D CNN as it can generate more features as compared to the 2-dimensional CNN using the CT images. The authors achieved the reduced false-positive ratio using the LUNA16 challenge dataset and achieved the highest CPM score.

Xie et al., [21] discussed a deep learning model to detect lung nodules at an early stage by separating the benign and malignant nodules from the computed tomography images. For accurate and early detection of lung cancer, malignant nodules accurate classification plays a vital role. Features of 3D lung nodules are learned by the developed model which results in 9 fixed views after the decomposition of the 3D lung nodule. After that, a collaborative sub-model based on the knowledge is constructed to represent each fixed view. Then based on the appearance, characterization of lung nodules is done using three pre-trained networks of ResNet-50 which are fine-tuned through the images patches of three types. Using back propagation, the classification of nodules is done using the updated weights. With a minimum effect on the proposed model, the ratio of false negatives is reduced using the penalty loss function. This proposed model achieved accuracy and AUC score of 91.60% and 95.70% respectively superior to other approaches for the classification of lung nodules using the LIDC_IDRI dataset.

Monkam et al., [22] defined a system to differentiate the non-nodules from the micro-nodules using computed tomography scan images. Here, a 3D convolutional neural network model has been proposed based on an ensemble learning technique. In this proposed system, the authors also addressed the false positive rate that is one of the major limitations in the earlier proposed systems. LIDC IDRI dataset has been used here containing 1010 CT images which further have 21315 non-nodules and 13179 micro-nodules image samples comprising a total of 34494 images samples. Five unique 3D CNN models against the five different-sized cropped nodules candidates

have been built and implemented in this study. The output of these models is then integrated with the extreme learning machine network for the final classification of the results. This system achieved the sensitivity, AUC, accuracy, and F-Score as 96.57%, 0.98, 97.35%, and 96.42% respectively. The results of this study are better than other 3D CNN and 2D CNN models and paved a way for micro-nodules study to detect lung cancer efficiently.

Kumar et al., [14] compared and implemented different algorithms for the CT images segmentation to boost the idea of automated segmentation without the intervention of the physicians. New and efficient segmentation algorithms are the need of time as images of large size are being generated which have some challenges that cannot be handled through the existing algorithms. In this study, authors analyzed and implemented five different algorithms with optimized performance to extract cancer from the lung images including guaranteed convergence PSO, k-median clustering, inertia-weighted PSO, k-means clustering, and particle swarm optimization. For the preprocessing stage of the CT images, a performance-based comparison is carried out here for the adaptive median, average, and median filters which proved the performance superiority of the adaptive median filter. An adaptive histogram equalizer is also applied here to enhance the contrast of the images. Here 20 lung images samples have been used for the validation purpose which provided the highest accuracy of 95.89% for the guaranteed convergence particle swarm optimization.

Kuo et al., [23] proposed an image processing technique in this paper for the lung nodules automatic detection from the computed tomography images. In this study, all nodule types have been considered for the detection and performed the steps including preprocessing of the images, segmentation of the lung images, enhancement of the lung nodules, detection of the lung nodule candidates, and false-positive ratio reduction. Support vector machines (SVM) have been applied twice in this study by the authors to reduce the false-positive ratio, while image accumulation is used to enhance the lung nodules. To process a single image, this system just takes only 0.1 seconds. A total of 667 lung nodules have been used in this study for implementation and evaluation purposes. This system achieved a 92.05% of overall sensitivity while 93.73% sensitivity was achieved by this system on the detection of 5mm-9mm lung nodules with reduced dales

positive ratio which demonstrates that this system can be used for rapid and accurate detection of lung nodules.

Abu Bakar and Ghadi [24] proposed a novel detection algorithm for the cancerous lung nodules from the computed tomography images using SVM and wavelet transform. This algorithm work in four different stages including the highlighting of suspicious regions using an enhancement algorithm, detection of the region of interest, and then in the 3rd and fourth stage, reduction of false-positive ratio is done using SVM and wavelet transform algorithms. For the evaluation purpose, 60 cases have been used here which resulted in a high sensitivity score for the cancerous lung nodules and achieved the false positive and true positive rate of 07 clusters per image and 94.5% respectively.

Wu et al., [25] proposed a dual branch network with an enhancement of the CT images for better segmentation of the lung nodules present in these images. Most related studies worked on the segmentation of the solitary lung nodules but to work on the non-solitary nodules is still a challenging task. In this study, authors also constructed and worked on their dataset which has non-solitary nodules. Moreover, the LIDC dataset has also been used for the segmentation of pulmonary nodules in this study. The authors suggested here a dual branch neural network with an images enhancement technique to fine the segmentation process of the lung nodules. In the image enhancement process, noise is removed from the images, lesion area is located and then boundary features are selected. For precise and accurate segmentation, U-net based dual branch network explores the 2D slices for more information and also investigates the 2D slices relationship with neighboring slices. This proposed approach effectively improves the learning of the network which eventually outperforms the related studies in this domain. The dice coefficient achieved by this proposed approach on the authors' dataset and LIDC dataset is 81.97% and 83.16% respectively.

Ozdemir et al.,[12] suggested a new diagnosis system for lung cancer that gives a meaningful probability assessment on the low dose computed tomography images. This proposed system performs detection of lung nodules as well as classification of the malignant nodules into 0 or 1 using a 3D convolutional neural network. Two publically available datasets have been used here including the Kaggle data science bowl challenge and Luna16. To eliminate the stage of false-

positive ratio and to improve the overall performance of the system, the authors considered here the coupling between diagnosis and detection components an important factor. A very first time for the CT images analysis, authors characterized the deep learning systems with model uncertainty that provided the calibrated probabilities for the classification task. The combination of these calibrated probabilities and model uncertainty can result in risk-based decision-making for the diagnosis phase and also can improve the results.

Cao et al., [26] addressed the problem of lung nodules detection due to their surrounding environment complexity and heterogeneity by proposing a 2-staged convolutional neural network. To detect the candidate nodules at an early stage, a segmentation-based network U-net with improvement has been used in the first stage. For training, a new sampling technique has been used in the first stage to reduce the false-positive ratio with a higher recall rate and a prediction method of two phases has been proposed as well. While in the second stage, to improve the false-positive ratio, a 3-dimensional CNN classification network with a dual pooling structure has been proposed. To increase the training sample size, a random mask has been used here by the authors as a data augmentation technique. Ensemble learning has been used here as well for the model responsible for false-positive ratio reduction with improved generalization ability. This proposed detection system achieved a competitive performance on the LUNA dataset.

In this study [27] authors first applied component analysis and region growing method to detecting the background of each 3 dimensional lung images. Then used a learnable 3D Maekov-Gibbs Random field approach which combined two visual sub-models and adaptive form prior sub-model to extract the suspicious area of lungs volumes and segment them into benign or malignant nodules. Furthermore, when enough hardware support is available, deep learning techniques can be used in this area including CNNs. Aresta et al., [28] proposed a deep learning model called iW-Net, which included lesion segmentation component and user intervention component. However, using a large size of nodules, the suggested system worked accurately without user involvement. Even, when intervention was added, the quality and of nodule segmentation was improved greatly in various non-solid and sub-solid abnormalities. In this study [29] authors, used 2&3 dimensional U-Net frameworks based on neural network for semantic lung segmentation using CT Scans. And, compare the efficiency result with Smart segmentation tools.

Zhao et al., [30] presented an end to end F-CNN to separate lung nodule in CT scan. Furthermore, a muti- instance loss (MIL) and adversarial loss methods are integrated with neural network to overcome the problem of segmentation in other pathological cases. In this work [31], authors combined both 3D-UNet and ResNet algorithm and design a new 3D-CNN known as 3D-Res2UNet for segmentation and detection of candidate pulmonary nodules. The updated Res2Net technique successfully resolve the expansion and disappearance gradient difficulties. The 3D-UNet network were applied to limited the size and recover the missing features map. In this study [32] authors, developed a new architecture called U-net convolutional network which segments lung regions from medical images.

In this study [33] authors, developed two model system called RU-Net and R2U-Net to segment different medical area of images including blood vessel, lung, and skin cancer segmentation. Both model were built on U-Net architecture. The suggest system provide better performance as compared to other similar network parameters such as Segnet, U-Net for segmentation job. The model were tested on LUNA16 image dataset and recieved 0.9918 % accuracy respectively. In this study [34] authors, developed deep learning-based U-Det framework for pulmonary nodule segmentation and added Bi-FPN between encoder and decoder as well. Furthermore, Mish function and class weight are utilized to increase nodule segmentation performance. The proposed model was validate on the LUNA dataset. A nodule segmentation approach's success can be judged in terms of accuracy, efficacy, robustness, stability, and level of automation [63].

In this work [35] authors, utilized intensity based thresholding in conjunction with morphological algorithm to segment and identify the elements and position of different lung nodules at the same time. Furthermore, cluster based classifier system showed good performance on a variety of independent databases and different modalities. In this study [36] authors, proposed system based Otsu's threshold method to detect and recognize different categories of CNDD including solid, part-solid, non-solid and juxrapleural lung nodules. First, Solid nodules are screened with stride 1. Secondly, threshold technique were used on each frame of window to locate candidate nodules. Finally, the logical OR operation were applied to merge all windows. Furthermore, muti-scale LoG filter integrate with Otsu's method to recognize pulmonary nodules.

In this paper [37] authors, used a combination of an intensity threshold and sizes of structural elements (SEs). The morphological opening method was performed by using six distinct intensity threshold (HU) values combine with radii of SEs: (− 400, 2), (−500, 2), (− 600, 2), (− 400, 3), (− 500, 3), (− 600, 3) for CNDD.

In this study Cascio et al., [38], presented 3-D mass-spring model to locate Candidate nodules. For accurate segmentation of lung volume, they used both region-growing and morphological algorithms. The range of gray values, as well as shape-related information from the proposed model, help to extract candidate nodules with maximum accuracy. In this work [39] authors, presented 2 & 3 dimensional deformable template matching and a genetic optimization algorithm to detect pulmonary nodule candidates. In this paper [40] authors, proposed a CAD system for detection and classification of cancer lesion. Initially, the thresholding approach was used to extract of lung parenchyma. Secondly, Gaussian filter were applied for enhancement and removal of noise from CT images. Furthermore, intensity and volumetric shape Index (SI) is employed to detect candidate nodules. Finally, a Fuzzy KNN algorithm was applied to classify nodules into malignant and benign.

Jiang et al., [41] discussed an efficient and automated lung nodules detection system for lung cancer better risk assessment. The quick and exact fix location of the lung nodules is a challenging task and many studies have proposed computer-aided systems to address this issue but these systems despite a higher number of image processing modules are not time efficient. Moreover, these systems except for some deep learning-based techniques suffer from the scalability problem as the data grow these systems cannot handle it efficiently. Based on multi-group patches an efficient detection CAD system for lung nodules has been developed in this study. These patches are cut from the images of lungs and further Frangi filter has been used for the enhancement of these images. To detect the four levels of the lung nodules and to learn the knowledge of the radiologists, a neural network model has been designed here based on the four channels and two groups of images. This proposed system attained 94% of sensitivity of 94% with per scan false positives as 15.1. While it achieved 80% of sensitivity with per scan false positives as 4.7. This proposed system is highly efficient for lung nodules detection and the reduction of FPs ratio.

In this paper Zheng et el., [42] addressed that radiologists did not use lung nodule detection systems on regular basis due to lack of performance and false-positive- ratio on different sizes of CT scan images. The authors proposed lung nodules detection system using deep learning CNN by providing multiple Maximum intensity projections (MIP) of various slab thicknesses. Two freely available datasets have been used here including LIDC/IDRC and LUNA 16. The proposed system reached a sensitivity of 92.7% with 1 FPs/scan and 94.2% with 2 FPs/scan. On small size, MIP images with 3mm -10mm the nodule detection system show fewer false-positive ratios. The proposed work is highly efficient for pulmonary lung detection whose size is more than 3mm and fewer false positives ratio. In this study [43] authors, provide DNN-based technique to detect candidate nodules. Firstly, an improved U-Net neural network was applied to extract the suspected lung nodules. Additionally, ResNet algorithm were combined with U-Net to increase the sensitivity performance of segmentation. Finally, VGG, Inception and Dense neural networks are combined called 3D multi-classification, to decrease false nodules.

In this research paper [44] authors presented a parallel neural network approach to segment lung nodules from CT images. The framework were based on hybrid attention system and DensNet algorithm. Additionally, the hybrid attention system combine spatial and channel attention module to overcome the complexity in pulmonary tumors and enhance its performance. Finally, different workable solution were implemented by adjusting the number of layer in the convolutions denseNet block. Huang et al., [45] provided an automatic framework to accurately separate pulmonary nodules from chest images. The framework were based on four elements, including 2 dimensional R-CNN to extract and identify pulmonary nodules, merging candidate lesions to reduce the irrelevant detection and improve accuracy, 2 dimensional CNN to correctly classify and decrease the FPs score, and upgraded VGG16 algorithm to segment nodule mask.

Suarez-Cuenca et al., [46], presented 3 dimensional region growing approach to effectively and precisely segment and detect nodule candidates using medical CT scan. After that, a parallel framework for classifier were developed including LDA, ANN, QDA and 3 SVM algorithm (SVM-dot, SVM-poly, SVM-ANOVA). The six component framework reduce the false nodules and show high sensitivity. Achieved, accuracy of 71.8, 75.5 and 80 percent at 0.8, 1.6 and 3.4 FPs per case respectively. El-Regaily et al., [47] initially applied contrast stretching to remove

unwanted noise from images. Secondly, multiple traditional approaches are used in combination such as 2D thresholding, morphological operation and 3D region growing, to segment lung nodules and to keep pulmonary tissues connected to the lung wall. Finally, Euclidean distance transform are used to detect candidates from ground truth.

In this paper Roy et al., [48] addressed that medical doctors did not use pulmonary nodule detection systems due to a lack of performance issues and false-positive ratio on different sizes of CT scan images. The authors proposed a detection system for pulmonary nodules using a machine learning fuzzy interference system. Firstly, the image contrast and binarization method were applied to remove noise disturbance from the CT scan. Furthermore, the active contour model extracted lung features and train the model on those features (area, boundary, length, width and mean) to classify cancer as benign or malignant. For nodule classification, a fuzzy interference technique was applied. This proposed system compared with SVM method and attained an accuracy of 94.12% respectively.

Mekali et al., [49] provided a fully developed automatic system to detect and separate JPNs. The ASSRGA and iterative thresholding algorithm were first implemented for the segmentation of lung parenchyma. Finally, CPBSCLLA and JPNs segmented methods were employed to segment the lung lobs and extract boundary images, hollow points and separation of connected thoracic from pulmonary nodules. Wu et al., [25] proposed here a dual branch neural network with an image enhancement technique to fine the segmentation process of the lung nodules. In the image enhancement process, noise is removed from the images, the lesion area is located and then boundary features are selected. For precise and accurate segmentation, U-net based dual branch network explores the 2D slices for more information and also investigates the 2D slices' relationship with neighboring slices. This proposed approach effectively improves the learning of the network which eventually outperforms the related studies in this domain.

In this study, Halder et al. [50] developed an automated computer-aided nodule detection framework. Firstly, Gaussian Mixture Model (GMM) method is used for nodule segmentation. Then, morphology filter were developed for vessel elimination and different intensity and shape-based characteristics are used for candidate nodule detection. Finally, to reduce the FPs we

employed SVM classifier of 10 cross fold validation approach and achieved 89.77 sensitivity against LIDC/IDRC dataset. Naqi et al. [51] proposed automated system for nodule detection and classification. Firstly, optimal gray level threshold used to extract lung region. Then, incorporated geometric texture and Histogram of Oriented Gradient decrease by principle Component Analysis (HOGPCA) features into a hybrid feature vector. Finally passed the extracted vector to k-Nearest Neighbor, Naive Bayesian, SVM, and AdaBoost to minimize FPs.

In this research paper [52] authors, developed a machine learning model to classify lung nodules at an beginner level by separating the benign and malignant candidate nodules from the computed tomography images. In preprocessing stage, authors eliminate background and surrounding tissue or vessels from lung nodules with help of thresholding and morphological operation. After that, priori information and Housefield Unit (HU) are used to measure the Region of Interest (ROI). Finally, for nodule classification SVM model were applied. Both shape and textural features are extracted and generated to train the classifier. The proposed model reached a sensitivity of 84.93% and accuracy of 78.08% respectively.

In this research paper [53] author, addressed the accurate detection of pulmonary nodules by developing a novel CAD system using 3-dimensional deep CNN framework with multi-scale prediction strategy from the CT images. In comparison to 2D CNNs, 3D CNNs are applied to automatically extract more lung features from volumetric images. Furthermore, Clustering and multi-scale small cubes are used to detect micro nodules. To validate the proposed system, the LUNA16 dataset has been used and gain a sensitivity score of 87.94% at 1 FPs/scan, 92.93 % at 4 FPs/scan. The proposed framework have some limitations like only used here volumetric medical image dataset and false nodules ratio increase when increase in sensitivity. In this study [54] author addressed the problem of nodule classification into cancerous and non-cancerous using CT scan images. Authors developed three different frameworks based on Convolutional Neural Network, DNN and Stacked Auto Encoder (SAE) for nodule classification. To increase the size of dataset author used flipping, translation and rotation techniques. Then trained the CAD system on the same dataset and generate the results. The experimental result shows that CNN performed well and achieved a sensitivity of 83.96% as compared to DNN and SAE.

Table 2.1: Comparison Table of Literature Review

Study	**Domain**	**Techniques**	**Weaknesses**
Changmiao Wanga et al., [16] (2017)	Machine learning	Cost-sensitive random forest (CS RF) + SVM	Not enough features to improve performance and used a small dataset
Gonzalez et al., [52] (2016)	Machine Learning	SVM	Prior information was needed for ROI extraction and false nodules ratio was high.
Roy et al., [48] (2015)	Machine learning	Active Contour Model + Fuzzy interference	Small size dataset are used and nodule classification is missing.
Nima Tajbakhsh et al., [17] (2017)	Machine learning and Deep learning	MTANNs + CNN	Limited training data
Xiaojie Huang et al.., [18] (2017)	Deep learning	3D CNN	The experiment was limited to cross-validation. Juxtapleural nodules were ignore.
Jia Ding et al., [19] (2017)	Machine learning and Deep Learning	Faster R-CNN + Three-dimensional DCNN	Slice thickness greater than 3 mm, not an accurate classification.
Qi Dou et al., [20] (2017)	Deep Learning	Multilevel Contextual 3D CNN	Suitable for only volumetric medical images
Gu et al., [53] (2018)	Deep Learning	3D deep CNN	Suitable for only volumetric medical images and GGN nodules are ignore
Yutong Xie et al., [21] (2019)	Deep Learning	multi-view knowledge-based collaborative (MV KBC)	Not enough features to improve performance. Only considered nodules ≧ 3mm
Monkam et al., [22] (2018)	Machine learning and Deep Learning	Ensemble 3D CNNs	Suitable for only volumetric medical images. Different models are used which slow down the performance and speed
Senthil Kumar et al., [14] (2019)	Machine learning	k-means clustering, Guaranteed convergence PSO with the adaptive filter	Only 20 Images are used
Kuo et al., [23] (2019)	Machine learning	Fast Otsu + Support vector machine (SVM)	Only considered nodules of size 5mm-9mm
Baker et al., [24] (2019)	Machine learning	Support vector machine (SVM)	Only used 60 CT images

Wu et al., [25] (2021)	Deep Learning	Dual Branch U-Net	Less training images
Ozdemir et al., [12] (2019)	Deep Learning	3D CNN	Fewer features representation and few features considered here
Cao et al., [26] (2020)	Deep Learning	U-Net and 3D CNN	Considered 3mm and larger size of nodules and ignored the nodules less than 3mm of size.
Jiang et al., [41] (2018)	Deep Learning	CNN	Only 3mm and greater than 3mm size of nodules are considered here
Zheng et al., [42] (2020)	Deep Learning	CNN	Consider 3mm larger size of nodules and ignored the nodules less than 3mm of size.

2.3 Summary

In this chapter, different techniques that have been implemented by different researchers are discussed. Some researchers have used just machine learning, some have used just computer vision techniques, some have used deep learning techniques while some have used hybrid techniques by combining two domains together such as the fusion of machine learning and deep learning. But we conclude that all the techniques that have been discussed above have their limitations. Some techniques are just limited to the CAD detection of lung nodules and some are just working on the classification of the nodules. While some techniques are just for the specific nodule size and ignore the different shape of small nodules. In all of these discussed techniques, there is a research gap in terms of small nodules detection and classification, false-positive ratio present in the results, less training images and bad accuracy.

CHAPTER 3

PROPOSED METHODOLOGY

3.1 Overview

This chapter presents the comprehensive discussion and details of the methodology that have been used to carry out the implementation part of this research work. From the dataset description, the preprocessing techniques that have been used to remove the noise and irrelevant information from the dataset, data augmentation techniques that have been used to enhance the dataset, deep learning model with a detailed architecture discussion and classification of the images are the part of this section.

3.2 Methodology

To address the above mentioned problems of accurate classification of lung nodules by considering the all sizes of nodules, I have proposed a deep learning based methodology involving deep convolutional neural network model. In this study, different models were considered to carry out this research work, but I have selected the one which was most suitable. In this research work, LIDC-IDRI dataset has been used which is one of the best resource in this area for training and testing purpose. In this methodology, preprocessing has been applied on the input images to remove the unwanted area and noise from the images. Then data augmentation technique has been performed to increase the number of images in the dataset as deep learning models require large size of dataset for better training and results generation. Different techniques are applied in data augmentation to increase the size of dataset. After that, deep learning model has been applied and

the images are fed to the model for training and texting purpose. Based on the set parameters, classification has been performed which tells us whether the image has cancerous nodules or not. An overview of the proposed architecture is given below in Figure. 3.1.

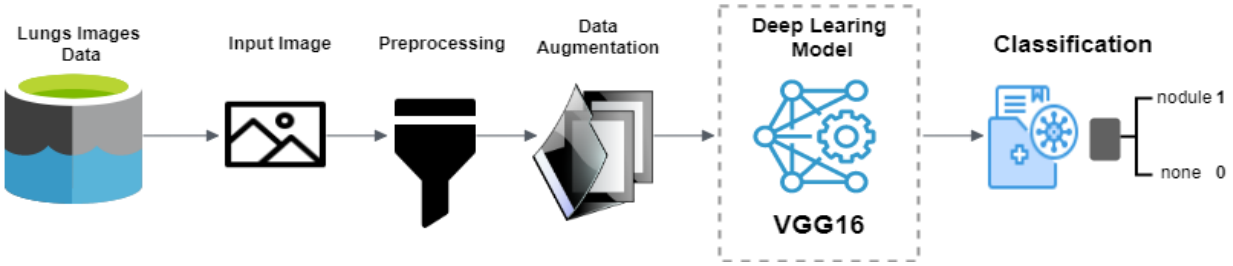

Figure 3.1: Proposed Architecture

From the above image, one can get an idea that how this research is being carried out? In this work, LIDC-IDRI database is used, which contains computed tomography (CT) images of Lungs cancer screening have been used. Annotations of this dataset are also given. Images from this dataset are first gone through the process of preprocessing in which, unwanted area of the images is cropped and then noise is removed from the images as both can have negative impact on the final output. After going through the preprocessing step, data augmentation technique is performed to enhance the size of sample images in the dataset. As a result, it will enhanced the training capacity of the deep learning model and make the image data in unbiased form. Furthermore, deep learning model perform well only when size of dataset is large. After that, pre-trained deep learning model VGG-16 is used both for training and testing purpose. This is used for classification and object detection purpose. This is one of the most recognized CNN based model to date which stands at number one in terms of object detection and number two in terms of classification on 1000 images of 1000 different classes and that makes it unbeatable till date. After applying the deep learning model, classification has been done considering all type of nodules from small sizes to large ones and also focusing on the reduced false positive ratio. In this work, images have been categorized into cancerous nodules images and images having no cancerous nodules. This research work involves following steps.

1. Acquiring lung nodules images data
2. Preprocessing

3. Data Augmentation
4. Deep Learning model
5. Classification

Step by step brief explanation of the above-given steps is given below.

3.3 Acquiring Lung Nodules Images Data

This is the first step towards the implementation of the methodology in which identification and selection of the proper dataset is the main task. As I have already mentioned that all sizes of lung nodules are being considered in this study, so I have also selected the LIDC-IDRI lung nodules images dataset which contains the CT scans of the lung nodules. It contains the annotations for each image as well as it is easily available and accessible. In this dataset, there are total 1018 cases of 463 unique images with a lateral and frontal projection which is the result of a collaboration of the public and private sectors including seven different academic institutions center and eight popular medical imaging companies with the input of food and drug administration (FDA) of USA. There is an XML file in the dataset containing the annotations of the images done by the four well-experienced thoracic radiologists. Each image has been examined by each experienced thoracic radiologist individually and together as well based on the following nodule size criteria:

Nodule $\geq$ 3mm
Nodule $\leq$ 3mm
$Non-nodule\ > or\ = 3mm A = \pi r^2$

Images in LIDC-IDRI database are in the DICOM format and cannot be opened through without proper application. To read these images, one will need a proper application which can read this type of file. The distribution of 463 unique images having cancerous nodules and non-cancerous nodules is given below in Figure 3.2

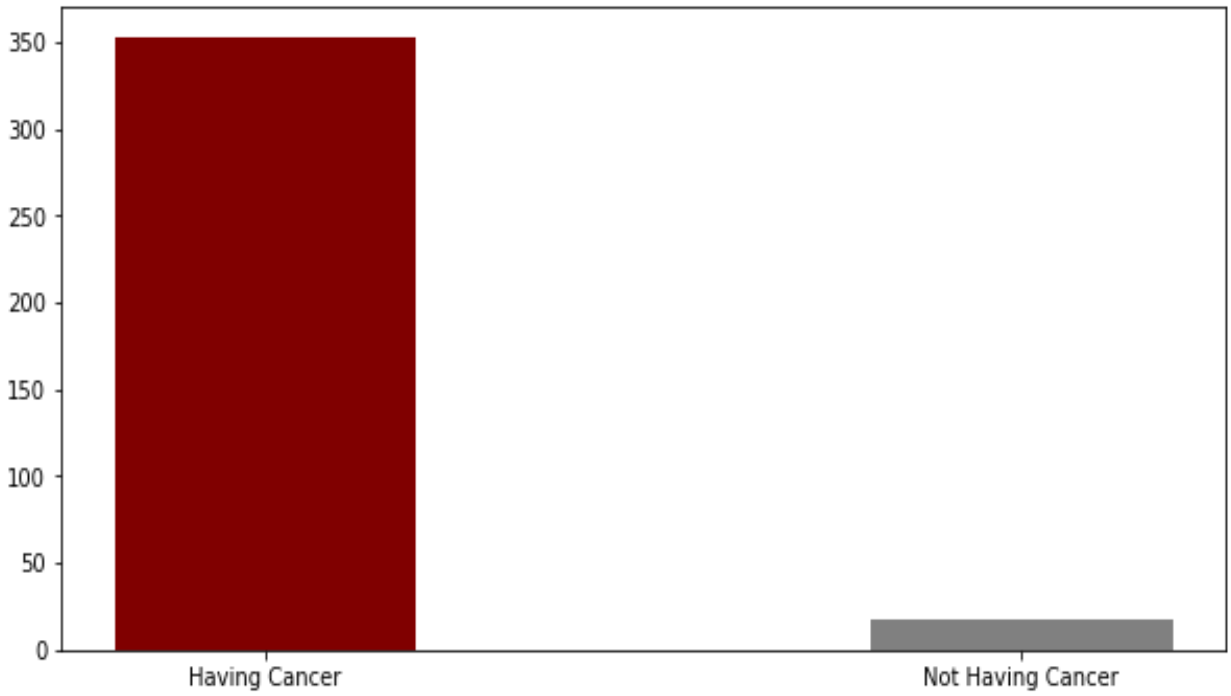

Figure 3.2: Distribution of images in cancerous and cancerous nodules

From the above-given figure, one can get an idea about the distribution of 463 unique images based on the cancerous and non-cancerous lung nodules which clearly shows that there is biasness in the distribution of data which is a serious concern and has been handled in the coming steps. The distribution of train and test images is also given below in Figure 3.3. Moreover, a screenshot of the XML file containing the annotations of each case and image is also given below in Figure 3.4.

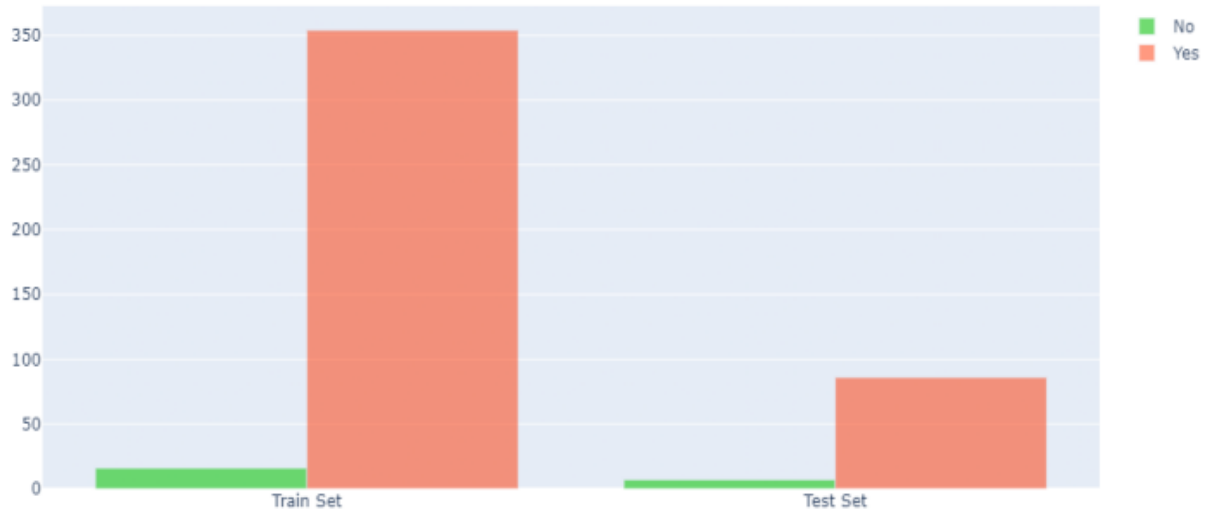

Figure 3.3: Distribution of train and test data

1	case_id	image_id	projection	findings
2	LIDC-IDRI-0001	LIDC-IDRI-0001-000001	Frontal	Nodules
3	LIDC-IDRI-0001	LIDC-IDRI-0001-000002	Lateral	Nodules
4	LIDC-IDRI-0003	LIDC-IDRI-0003-000001	Frontal	Nodules
5	LIDC-IDRI-0003	LIDC-IDRI-0003-000002	Lateral	Nodules
6	LIDC-IDRI-0004	LIDC-IDRI-0004-000001	Frontal	Nodules
7	LIDC-IDRI-0005	LIDC-IDRI-0005-000002	Lateral	Nodules
8	LIDC-IDRI-0005	LIDC-IDRI-0005-000001	Frontal	Nodules
9	LIDC-IDRI-0006	LIDC-IDRI-0006-000002	Lateral	Nodules
10	LIDC-IDRI-0006	LIDC-IDRI-0006-000001	Frontal	Nodules
11	LIDC-IDRI-0007	LIDC-IDRI-0007-000001	Frontal	Nodules
12	LIDC-IDRI-0007	LIDC-IDRI-0007-000002	Lateral	Nodules
13	LIDC-IDRI-0008	LIDC-IDRI-0008-000002	Lateral	Nodules
14	LIDC-IDRI-0008	LIDC-IDRI-0008-000001	Frontal	Nodules
15	LIDC-IDRI-0010	LIDC-IDRI-0010-000001	Frontal	Nodules
16	LIDC-IDRI-0011	LIDC-IDRI-0011-000000	Frontal	None
17	LIDC-IDRI-0011	LIDC-IDRI-0011-000001	Lateral	None
18	LIDC-IDRI-0012	LIDC-IDRI-0012-000002	Lateral	Nodules
19	LIDC-IDRI-0012	LIDC-IDRI-0012-000001	Frontal	Nodules
20	LIDC-IDRI-0013	LIDC-IDRI-0013-000001	Frontal	Nodules
21	LIDC-IDRI-0013	LIDC-IDRI-0013-000002	Lateral	Nodules
22	LIDC-IDRI-0014	LIDC-IDRI-0014-000001	Frontal	Nodules
23	LIDC-IDRI-0014	LIDC-IDRI-0014-000002	Lateral	Nodules
24	LIDC-IDRI-0016	LIDC-IDRI-0016-000001	Frontal	Nodules
25	LIDC-IDRI-0016	LIDC-IDRI-0016-000002	Lateral	Nodules
26	LIDC-IDRI-0018	LIDC-IDRI-0018-000001	Frontal	Nodules
27	LIDC-IDRI-0018	LIDC-IDRI-0018-000002	Lateral	Nodules
28	LIDC-IDRI-0019	LIDC-IDRI-0019-000001	Frontal	Nodules

Figure 3.4: Data annotations for each case and image given in XML file

3.4 Preprocessing

Preprocessing is a crucial phase in the study of lung CT scan. It aims to improve image resolution, quality and also remove unwanted information (noise, artefacts, etc.) from the raw images, to get better outcomes in the diagnosis of lung nodules. Furthermore, preprocessing can improve the ability of nodule detection to maximize and simplify valuable information. In this study [55] authors, effectively extracted the lung region using a variety of preprocessing approaches, such as connected component labelling, hole filling, and optimal gray-level thresholding. Manickavasagam et al., [56] used a Gaussian filter to remove noise and improve delay in medical image processing. In this research study, [57] authors, use three preprocessing techniques for medical images based on top-hat transformation, median, and adaptive bilateral filter. The bilateral filter gives better results as compared to the other two techniques. In this study [58] authors, initially employed Gaussian filter, method of thresholding and intensity to remove the mask of pulmonary nodules and filter out other regions (organs and tissues), and then applied morphological method based on convex hull computing and dilation to maximize mask separation. Figure. 3 draw out a complete step-by-step explanation of preprocessing approach.

This is the 2nd step of the methodology in which excessive or unnecessary area present in the images have been cropped to remove the noise from the images and also blurred images or subjective area have been stored by applying a threshold on the images so that area under the examination should be there with clear vision. Moreover, image resizing is also the part of this step in which images have been resized. Preprocessing helps to gain better and unbiased results as factors that mostly affect the results are removed in this process.

In the below given Figure 3.5 from left to right, an original scan image from the dataset is given which has an unnecessary area in the figure which should needs to be removed. The right side of image is the result of the cropping which is the part of preprocessing to remove the excessive area from the original image so that only that part should be considered which contains the subjective area or which deems to be necessary.

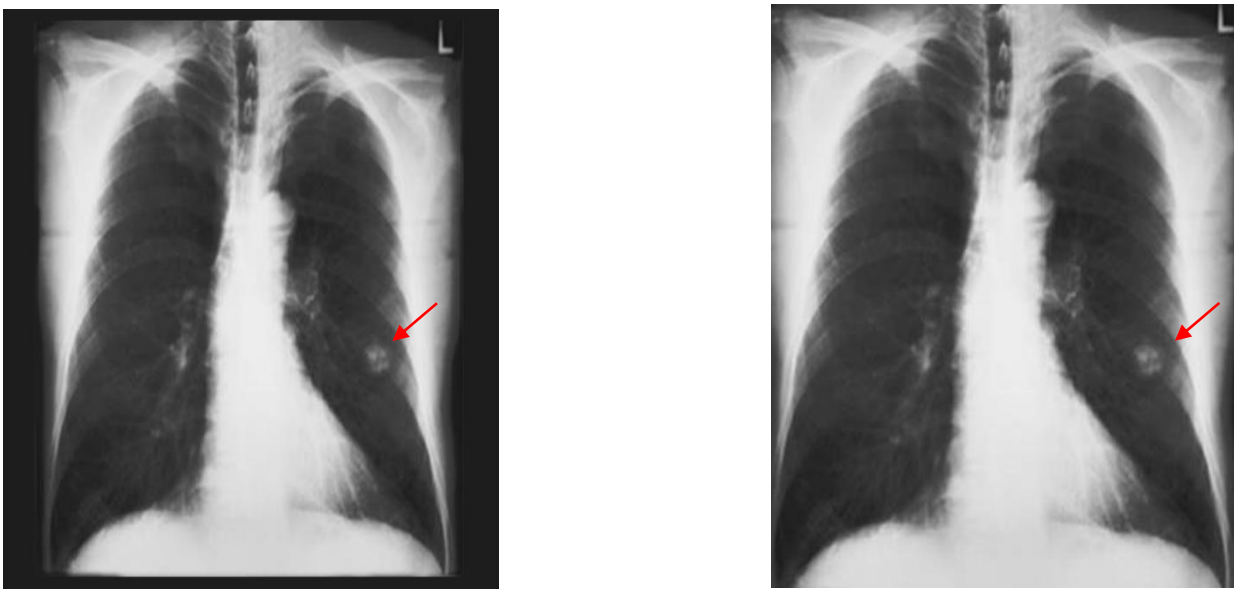

Figure 3.5: Actual image and a preprocessed image after cropping

In the below given Figure 3.6 from left to right, the problem of different color intensity and blurriness of the image is addressed. At the start, images have been converted into grayscale, and then applying a preprocessing technique of threshold to find out the exact edges of the images or smooth the images.

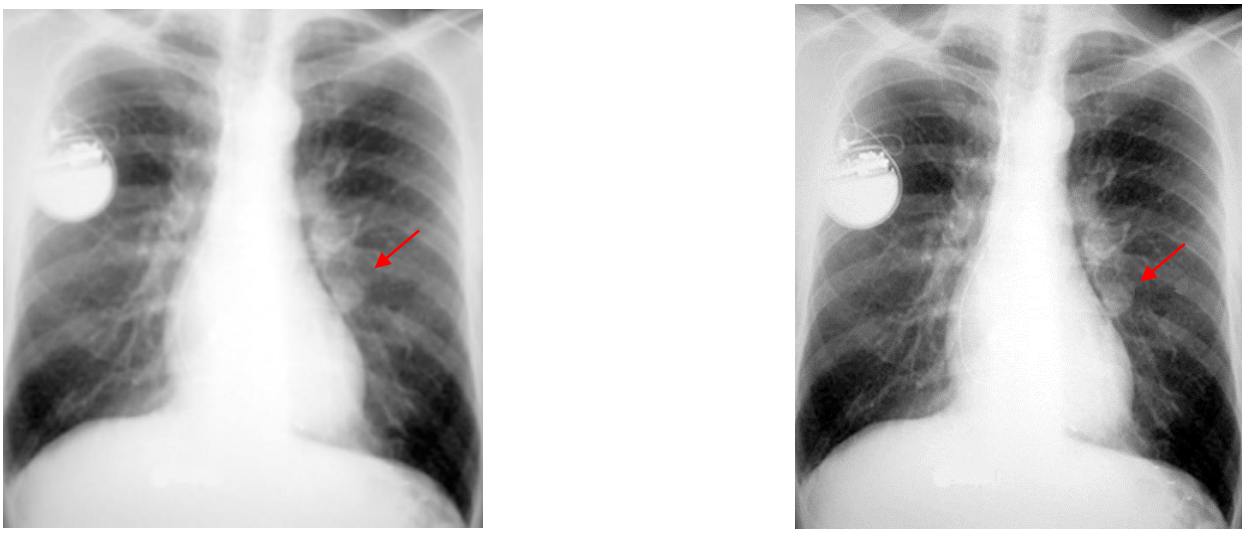

Figure 3.6: Blurred image on left side and smooth image after preprocessing on right side

3.5 Data Augmentation

Augmentation of data is the 3rd step of the methodology in this research study in which different augmentation methods such as horizontal rotation and vertical rotation and flipping of image as well as rotation of image from 0 to 180 degree to increase the size of dataset. As those images which have non-cancerous nodules are very low in size, so data augmentation technique is applied on such type of images to remove the biasness from the data and to increase the size of very low images. This technique has also been used by many researchers in different studies to balance the data. Figure 3.7, given below depicts the different data augmentation technique applied on a preprocessed image.

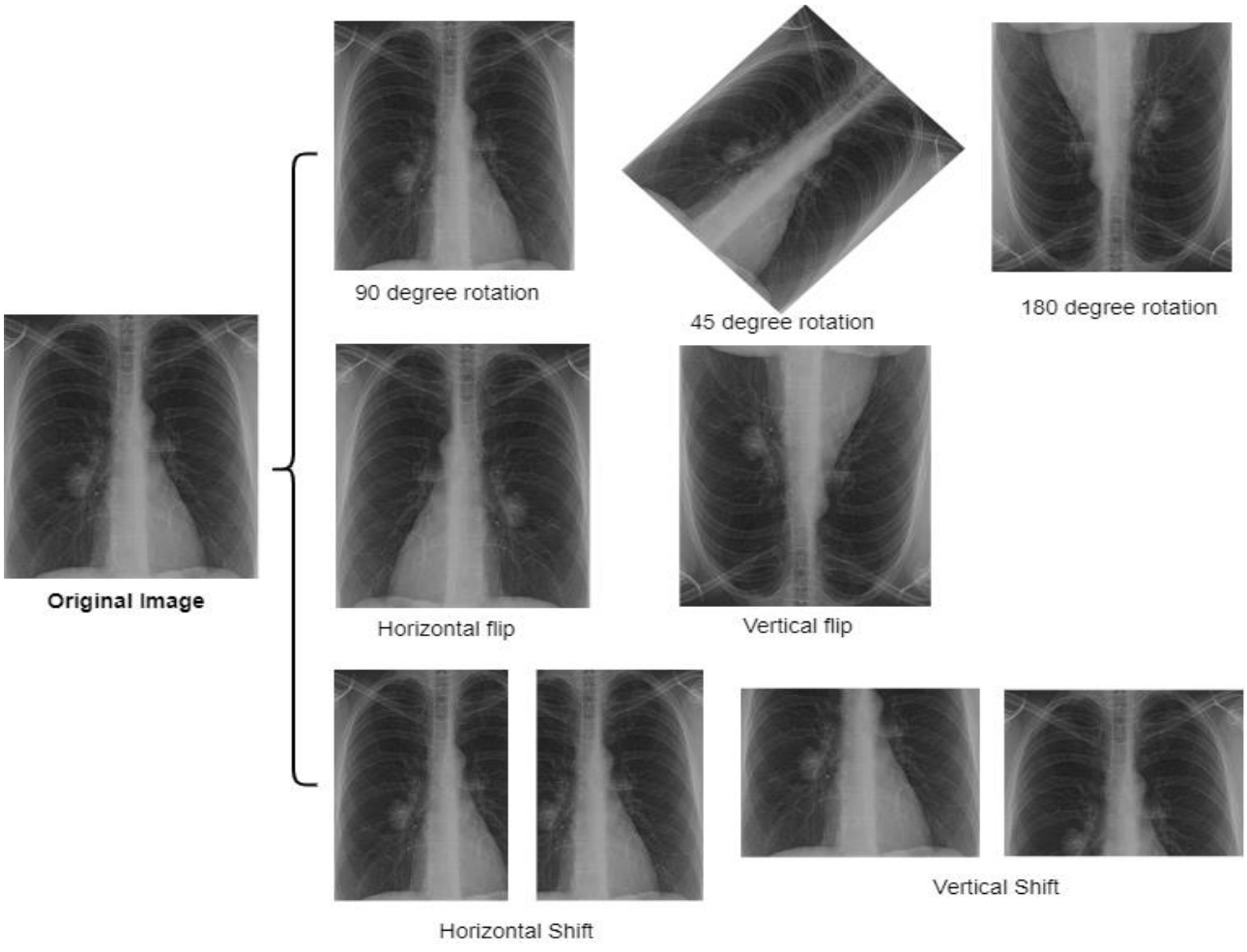

Figure 3.7: Different data augmentation techniques applied on the images

From the above given image, one can see that three data augmentation techniques have been applied including image rotation from 0 to 180 degree, horizontal and vertical flipping and shifting of the image so that dataset size can be increased.

3.6 Deep Learning Model

In this step, deep learning based model has been used. In this study, a convolutional neural network based VGG16 model is used which is pre-trained on ImageNet dataset that has 1000 classes and each class contains 1000 images. So, a fine tuned VGG16 model has been used with hyper parameters tuning. In this study, some other deep learning models have also been tested but due to higher false positive ratio and average accuracy, such models have been removed from this study. In this step, VGG16 has been used for both training and testing purpose and for this purpose augmented dataset has been divided into train and test data in a ratio of 75% train data and 25% test data. Overall architecture of VGG16 has been discussed below in sub-section 3.5.1.

3.6.1 VGG16 Architecture

VGG16 model was first presented in an ImageNet challenge in 2014 by a team of University of Oxford for the object detection and classification. It is based on convolutional neural network which has an input layer, some hidden layers and an output layer. This model has total of 21 layers in it while there are 16 weight layers in it. There are total thirteen convolution (Conv.) layers, three dense or fully connected (FC) layers and five pooling layers.

It takes an image as an input with 3RGB channels and a tensor size of 224x224. After input layer, there are two convolution layers having 64 filters followed by a pooling layer, then two convolution layers having 128 filters followed by a pooling layer and then three convolution layers having 256 filters followed by a pooling layer. There are aging three convolution layers having 512 filters followed by a pooling layer and then three more convolution layers having 512 filters

followed by a pooling layer. After that, there are three dense or fully connected (FC) layers, rectified linear unit (Relu) has been used here as an activation function with a learning rate of 1e-4. While at the end there is output layer with softmax as an activation layer for the classification of objects. Moreover 4096 channels have been used in the first two dense or fully connected layers and 1000 channels for a 1000 class problem have been used in the last dense or fully connected layers just before the softmax activation layer. In this architecture there are convolution layers of 3x3 filter having a stride of 1 and a dropout layer has also been used by me with a value of 0.5. The overall architecture of VGG16 is illustrated below in Figure 3.8.

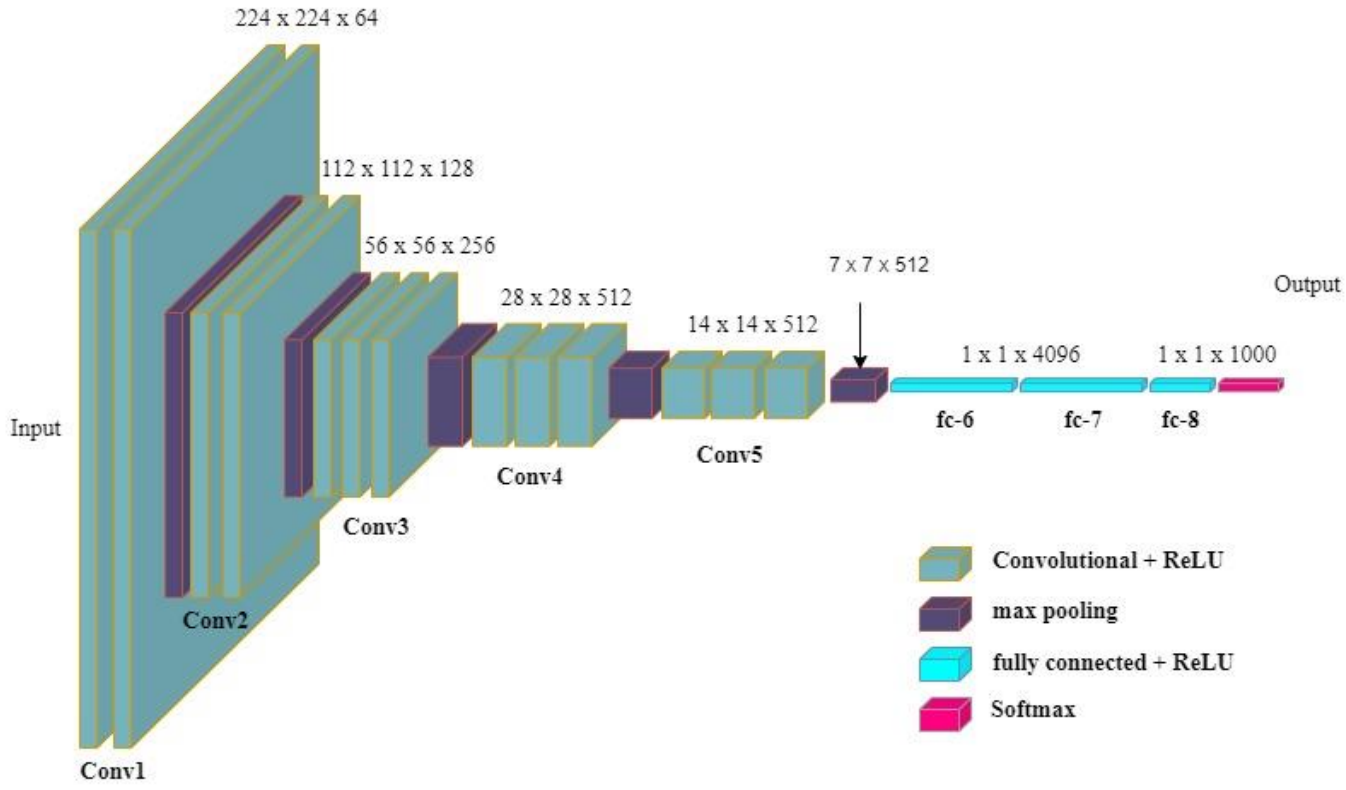

Figure 3.8: VGG16 architecture

The overall architecture of VGG16 that has been used in this study and in the implementation work is also shown in the below given Figure 3.9 in which it is mentioned that this model will classify the images into two classes and is a sequential model as convolutional pooling layers are in a sequence and the summary with trainable parameters is shown in Figure 3.10

```
NUM_CLASSES = 2

model3 = Sequential()
model3.add(base_model2)
model3.add(Flatten())
model3.add(Dense(1024, activation = 'relu'))
model3.add(Dense(512,activation = 'relu'))
model3.add(Dense(256,activation = 'relu'))
model3.add(Dense(128,activation = 'relu'))
model3.add(Dropout(0.5))
model3.add(Dense(NUM_CLASSES, activation='softmax'))
```

Figure 3.9: VGG16 architecture in implementation work of this study

```
[ ]
model3.summary()
```

```
Model: "sequential"
_________________________________________________________________
 Layer (type)                Output Shape              Param #
=================================================================
 vgg16 (Functional)          (None, 7, 7, 512)         14714688

 flatten (Flatten)           (None, 25088)             0

 dense (Dense)               (None, 1024)              25691136

 dense_1 (Dense)             (None, 512)               524800

 dense_2 (Dense)             (None, 256)               131328

 dense_3 (Dense)             (None, 128)               32896

 dropout (Dropout)           (None, 128)               0

 dense_4 (Dense)             (None, 2)                 258

=================================================================
Total params: 41,095,106
Trainable params: 41,095,106
Non-trainable params: 0
```

Figure 3.10: Summary of the VGG architecture with total parameters and trainable parameters

3.7 Classification

In this last step, the classification of the lung nodules have been performed into two classes, cancerous nodules images represented by 1 and non-nodules images represented by 0.

3.8 Summary

In proposed methodology chapter, the overall architecture of the implementation work has been illustrated through a figure and presents a detailed information and discussion. Preprocessing and data augmentation techniques have been explained using the figures illustration which makes it easy to understand that how these techniques have been actually applied on the dataset. Moreover, VGG16 model has been discussed in such a way that each layer has been explained with their functionality and an illustrative figure makes it easy to understand. Moreover, how classification has been done is also explained.

CHAPTER 4

TECHNICAL BACKGROUND & EXPERIMENTAL SETUP

4.1 Overview

It is vital to have proper knowledge of machine learning (ML) and its various learning concepts. In order to develop accurate and efficient CAD system using deep learning network. Therefore inside technical background section I will first explain the machine learning basic theory and then explain all other essential components in order to solve the problem which is related to deep learning. The Experimental environment setup section I have discuss that how implementation part has been actually done. In this chapter, specifications of the hardware used, programming language with version, libraries that have been used and different evaluation metrics that have been used to measure the results.

4.2 Technical Background

4.2.1 Machine Learning

Computers are built on the basic arithmetic operation and logical gate and follow binary language instruction to solve a particular task. Daily activities that are simple for human beings, such as identifying automobiles and faces, are tremendously tough for robots. A machine might be used to handle such kind of problem by developing an algorithm or giving a set of instructions that inform the machine how to process the input data to produce an output result. In some cases,

it will be tough to develop an algorithm if the problem is too complex. This sparked the concept of creating machines that could learn by themselves and solve problems without being given explicit instructions. This is known as Machine Learning (ML). The concept is based on how people learn. To be able to distinguish between dogs and cats, we will need to observe a lot of example data and be notified which things are cats and which are dogs. We would gradually learn unique cat and dog characteristics by repeating this a dozen times, allowing us to differentiate between them afterward. Figure 4.1 below show the AI-ML-DL spectrum and its relationships.

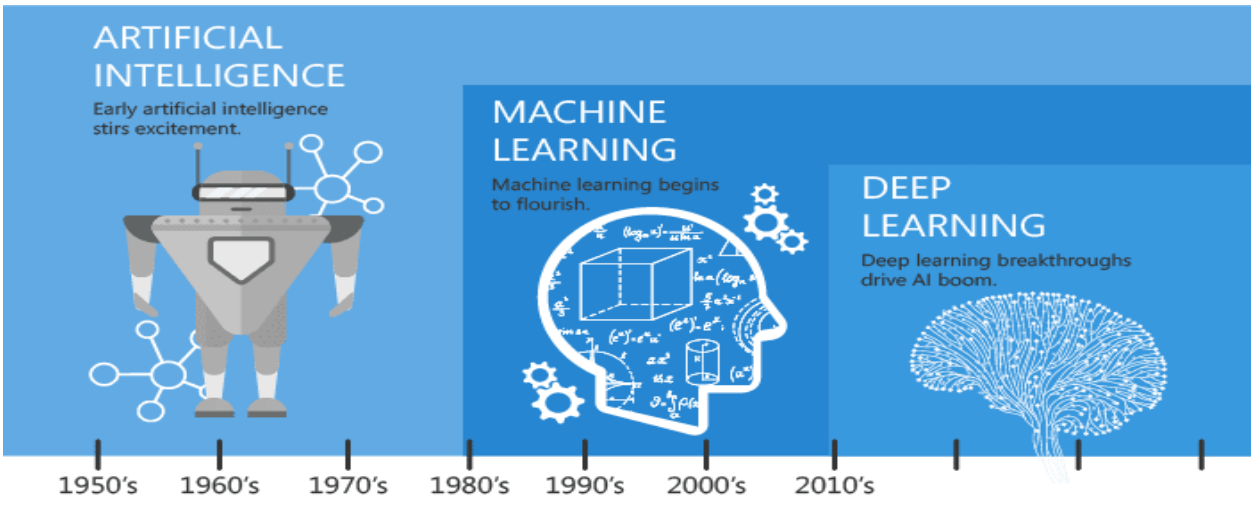

Figure 4.1: Show range of AI, ML, and DL, and how they are related to one another [59].

Machines are now able to imitate human cognitive capabilities because of the introduction of this learning idea and problem-solving capacity. This is referred to as Artificial Intelligence (AI). ML is a branch of AI that solely deals with learning-based ideas. Deep Learning is a machine learning subcategory (dl). It is founded on the idea that data has a hierarchy of complexity. By learning increasingly complicated characteristics from the incoming data, the computer is able to tackle more difficult problems

Supervised Learning: The three sub-categories of machine learning are as follows: supervised, unsupervised and semi-supervised. Supervised learning uses labeled data to train the machine learning model. Even though precise data labeling is required for this approach to

function, supervised learning is highly effective when applied in the correct situations. Unsupervised machine learning in which algorithms are trained without the use of ground truth. Semi-supervised machine learning is based on both labeled and unlabeled data, although in most cases, data is unlabeled. This kind of learning is a hybrid of supervised and unsupervised learning.

Theoretically, supervised learning would always outperform unsupervised learning if enough annotated data were provided. However, for supervised learning to generalize well, a large amount of labeled data is required. As a result, in certain circumstances, unsupervised methods, like image segmentation, may be more appropriate. In order to achieve excellent performance on complex problems then supervised learning techniques are applied.

4.2.2 Deep Learning

The field of machine learning now includes deep learning. It uses artificial neural networks ANN, a type of computing system with biological factors. Deep learning methods are now widely utilized in bioinformatics, speech recognition, audio recognition, natural language processing, and image processing. In a few of these domains, the results are on par with or even superior to those obtained by human specialists [60]. Traditional machine learning techniques, such as support vector machines and shallow neural networks, have a number of drawbacks that deep learning methods do not. The primary benefit is that deep learning algorithms are able to automatically extract the features from the data. As a consequence, there is no requirement for the participation of humans in the training process. In addition, this feature extraction technique creates characteristics that are challenging for a person to conceive of and apply.

4.2.3 Artificial Neural Networks

An artificial neuron network is a sub-field of artificial intelligence that imitates the way nerve cells function in the human brain. The idea of ANN is founded on our understanding of the

basic nature of the brain. Humans base their decisions on a variety of criteria and inputs, which they weight in some way before reaching a final decision. Each of these inputs is referred to as a neuron, which is interpreted similarly in neuroscience. The perceptron, often known as a single-layer perceptron, is the simplest basic type of neural network. When we talk about a layer, we're referring to a group of neurons that receives variously weighted outputs from a related group of neurons before. The input layer, which includes the input data to be processed, is one example of a layer. Multilayer neural network structure pic is given below in figure 4.2.

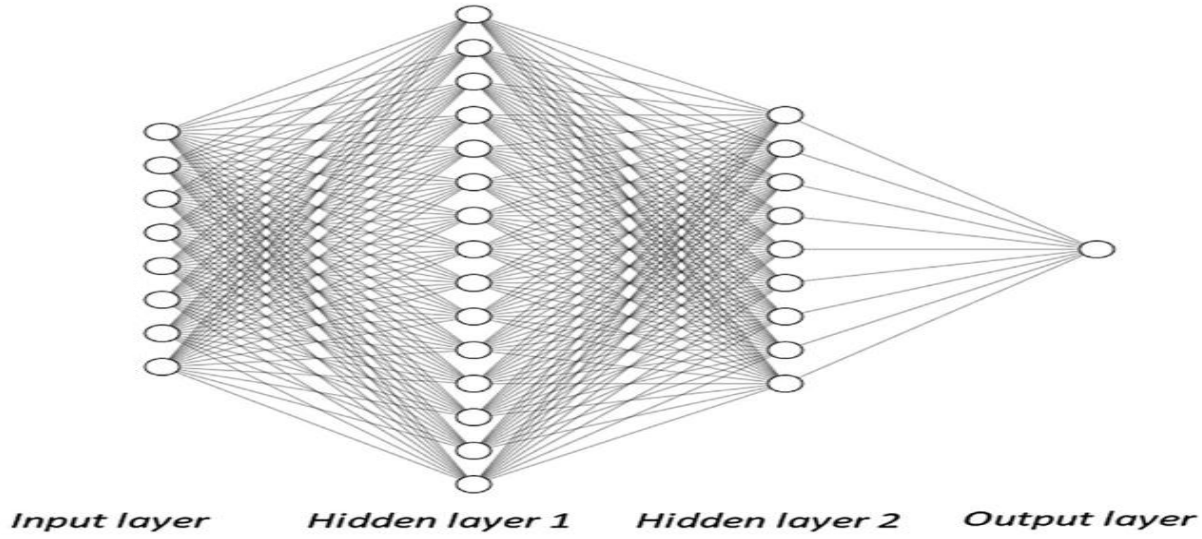

Figure 4.2: Show an example of a multilayer neural network. In this instance, the perceptron consists of three layers [61].

A single-layer perceptron may be conceptualized as the dot product of an input x and a set of weights w, with the addition of some bias term w0 to produce:

$$y = \mathrm{w}^{\mathrm{t}}\,\mathrm{x} + w_o \sum_i w_o\, x_i + w_o \qquad 4.1$$

This transformation is linear. The single-layer perceptron is hence referred to as a linear classifier. It accepts some input value (x) and uses a linear transform to classify the output to a certain value (y). If the desired output falls within a certain range, such as y [0, 1], it could be useful to employ an activation function, such as:

$$y = \int (\mathrm{w}^{\mathrm{t}}\,\mathrm{x} + w_o) = \int (g(x)) \qquad 4.2$$

The resultant classifier is nonlinear for any nonlinear activation function. Below figure 4.3 represent the difference between linear and non-linear function

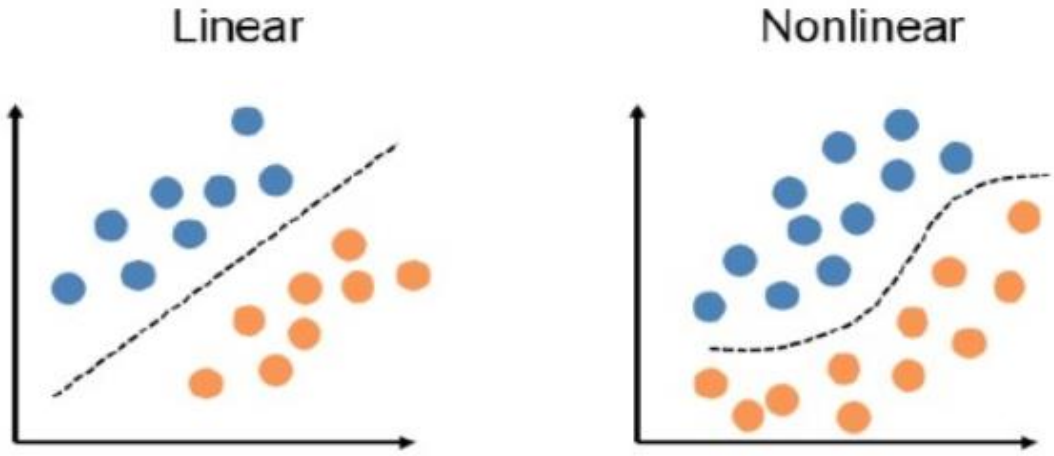

Figure 4.3: Difference between linear and nonlinear boundary function

The assumption made when using a linear classifier is that a linear border function g may be used to divide the classes into data. Nonlinear classifiers are frequently used for real-world applications because they may generalize more effectively and be able to tackle more challenging issues. When dealing with increasingly difficult issues, it's possible that you'll need to employ additional layers in order to produce more complex border functions. Hidden layers are the name given to these additional levels. More complex mappings may be created by adding more layers. It is possible to create more advanced mappings by inserting more layers. The data is changed such that in the converted domain it can be more easily separated along linear lines, but in the original domain, it seems to be some kind of complex border function.

Architecture is the collection of resultant layers of neurons. It specifies how the data is handled in order to provide the desired results. If we were to classify the image of cars and trucks, a suitable measure for assessment would be the accuracy of the classification, which would be defined as the number of cars and trucks that are properly identified. However, how can we truly maximize the accuracy of the classification? This is accomplished by determining the best

combination of weights for the network under consideration. Backpropagation is the process that teaches the network how to adjust the weights. So that it can provide the best possible output, and it is the mechanism that is used to choose them.

A cost function or loss function j is required to employ backpropagation. Its main work is to control the weights settings. The loss function may be increased or decreased depending on the selected loss function. The Sum of Squared Error (SSE) loss is one type of loss function, and it is defined as below in equation 4.3. Where yi represents the observed value, yˆi predicted class and n sample.

$$Jsse = \sum_{i=1}^{n} (y_i + \hat{y}_i)\, 2 \qquad 4.3$$

If the sum of squares error (SSE) is low, it means that the overall observed value y and the predicated value are comparable, reflecting the desired outcome. Indicating that the desired result was achieved. As a result, this loss function is used as a classifier.

4.2.4 Backpropagation

The most important part of training a neural network is called backpropagation. It is the process of fine-tuning the weights of a neural network depending on the error rate achieved in the preceding epoch of the network's training (i.e., iteration). By fine-tuning the weights in the right way, it is possible to lower the overall error rate and improve the model's reliability by expanding its applicability. The term "backward propagation of errors" can be shortened to "backpropagation," which is used in neural networks. It is a strategy that is commonly used for training artificial neural networks. Calculating the gradient of a loss function with respect to all of the weights in a network is made easier by using this approach.

Within a neural network, the Back propagation algorithm is responsible for computing the gradient of the loss function for a single weight using the chain rule. In contrast to a native direct

calculation, it computes just one layer at a time, but it does it in an efficient manner. It conducts the computation for the gradient, but it does not describe how the gradient should be used. The computation that is found in the delta rule is made more generic by this. Take a look at the back propagation neural network sample diagram in Figure 4.4 that follows to get a better understanding:

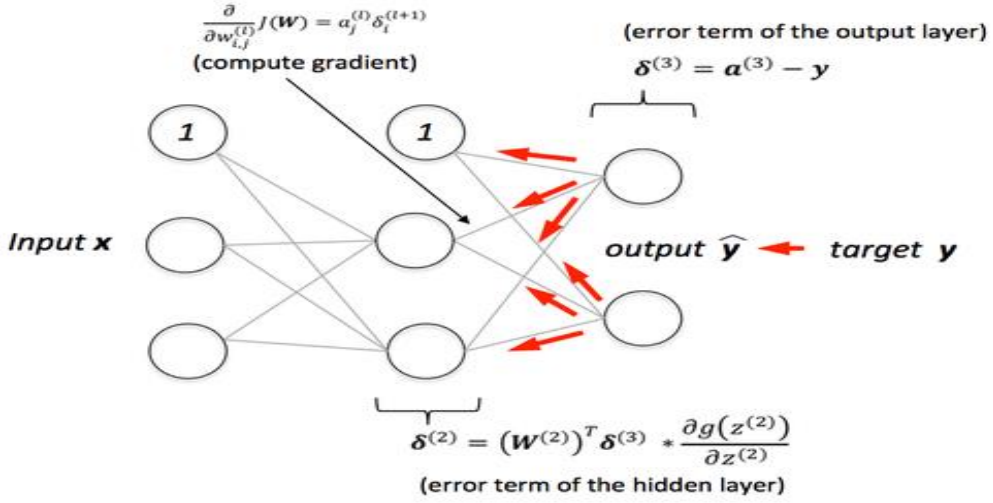

Figure 4.4. Back propagation neural network diagram [62].

4.2.5 Gradient Decent:

Gradient descent, which is the idea that is commonly utilized in backpropagation, is the most common and widely used method for improving neural networks [63]. When we speak of optimizing a neural network, we are referring to the process by which the network does an iterative search for a loss function that has a lower minimum (or a larger maximum). If a greedy approach were taken (only accept the solution if lower minimum for each iteration), the optimization may become mired in a local minimum. As a result, it is essential to make use of a strategy that is more advanced.

The process of gradient descent is a method for minimizing any arbitrary (loss) function j (θ) that is parameterized by the model θ $\in R^d$, where d refers to the dimension. This is achieved by changing the parameters θ in the inverse direction of the loss function's gradient with respect to θ.

During this phase of the descent, it is required to define a **learning rate** (LR) denoted by the symbol μ. This LR determines the total number of iterations that must be performed in order for the function to arrive at a (local) minimum. One further way of looking at it is to determine how much weight should be placed on newly acquired information. If you use a value that is too small for μ, training might be sluggish and it could become mired in a local minimum. If you choose a greater value for μ, it has the potential to leap over these smaller local troughs, but it also has the potential to exceed the optimum.

As previously discussed, there is a significant connection between gradient descent and backpropagation. The resulting updating technique may be described mathematically as follows [64]:

$$w_j^r(\text{i} +1) = w_j^r(i) - \mu\nabla \text{w j(w)} = w_j^r(i) - \mu\delta_j^r(\text{i})\, y^{r-1} \qquad 4.4$$

The technique for upgrading is carried out on many occasions. In an iterative process, the training data are added to the network until either the algorithm converges or it reaches a predetermined stopping point. An **epoch** is a term used to describe each subsequent forward-backward propagation of all of the training data.

As a method of regularization, performing updates on a more frequent basis might prove to be beneficial. As a consequence of this, it is common practice to partition the data into smaller chunks and then update the model after each of these **chunks.** This could potentially speed up the training process while also improving the system's ability to find better minima.

4.2.6 Optimizer

Optimizers are techniques or approaches that are applied to minimize an error or loss function and to enhance production accuracy. Optimizers are mathematical calculations that are reliant on the weights and biases, two learnable parameters of the model. Optimizers assist in determining how to adjust the weights and learning rate of a neural network in order to minimize losses.

Adam Deep Learning Optimizer: The word Adam comes from adaptive moment estimation. This optimization method updates network weights during training by extending stochastic gradient descent. Adam optimizer modifies the learning rate for each network weight separately, unlike SGD training, which maintains a single learning rate. The designers of the Adam optimization technique are aware of the advantages of the AdaGrad and RMSProp algorithms, which are also stochastic gradient descent extensions. As a result, both the Adagrad and RMS prop algorithms characteristics are inherited by the Adam optimizers. Adam employs both the first and second moments of the gradients to adjust learning rates rather than just the first moment (mean) as it does in RMS Prop. The uncentered variance is defined as the second moment of the gradients.

Because of its many advantages, the Adam optimizer is frequently utilized. It has been modified to serve as a benchmark for deep learning publications and is suggested as a standard optimization approach. More so than any other optimization technique, the algorithm is simple to develop, runs more quickly, uses less memory, and needs less adjusting. The operation of the Adam Optimizer is represented by the formula below. Here, B1 and B2 stand in for the average gradient's decay rate [65].

$$mt = \beta_1 m_{t-1} + (1- \beta_{1)\, gt} \left[\frac{\delta L}{\delta w_t}\right] \qquad 4.5$$

$$vt = \beta_2 v_{t-1} + (1- \beta_{1)} \left[\frac{\delta L}{\delta w_t}\right]^2 \qquad 4.6$$

4.2.7 Loss Function

The loss function is the function that determines the difference in value between the actual output of the algorithm and the predicted output of the algorithm. It is a technique for determining the accuracy of the data models produced by your algorithm. It is possible to divide it up into two different categories. One for classification (with discrete values such as 0, 1, 2, etc.), and the other for regression (continuous values). In the training stage of neural networks, selecting the appropriate loss function is crucial for obtaining the best results. The loss function used is determined on the job. SSE may be a useful option for classifying autos and trucks, as was stated in section 2.2. Despite being straightforward, it has its drawbacks, such as issues with tiny gradients.

Another problem that may arise during training is that the various categories may not be represented in an equal manner for example the image of cars is more as compared to another category (dogs). If we were to train a dog/cat classifier based on this data set and use basic SSE as the loss function, the network would most likely only end up predicting cats. The rationale for this is that if you choose a cat every time, you will make fewer mistakes than if you guess a dog. As a result, it receives an inappropriately severe penalty in the dog class but an inappropriately light penalty in the cat class.

Before beginning any sort of training, it is necessary to address the issue of imbalanced data sets. Either resampling the data in such a way that they are balanced throughout training or making use of a loss function that weights and penalizes classes in the appropriate manner during training. Unbalanced data sets are more challenging to segment since it is harder to physically balance the classes. To deal with the imbalanced data sets during training in this situation, it could be required to include a loss function.

Cross- Entropy Loss Function: Loss/cost functions are used to optimize the model during training while working on a machine learning or deep learning problem. The goal is often to reduce

the loss function. The better the model, the lesser the loss. A crucial cost function is a cross-entropy loss. It is employed in the optimization of classification models.

Figure 4.5. Assume a four-class classification problem and classified the input image into a cat, dog, horse, and cheetah respectively

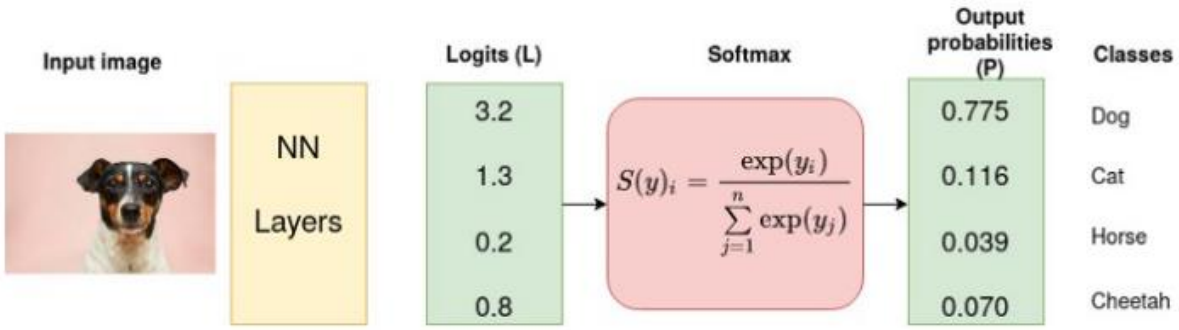

Figure 4.5: Show the structure of cross-entropy loss function with help of 4 class classification example [66].

In the figure given above, the softmax activation function converts logits into probabilities. The objective of the Cross-Entropy is to note down the output probabilities of the model and then calculate the difference between the actual values and the model-generated output value (below-given figure).

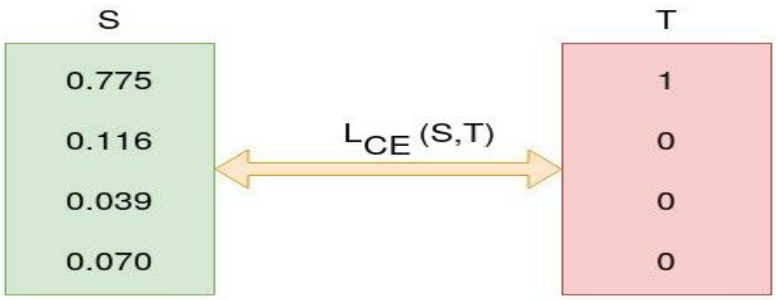

Figure 4.6: Softmax function converts logits into probabilities [66]

The above example indicate that the expected result for dog class [1, 0, 0, 0], however the model generate [0.7775, 0.116, 0.039, 0.079]. The goal here is to get the output of the model to be as near to the expected result (truth values). The model weights are repeatedly modified during model training in order to minimize the Cross-Entropy loss. Model training is the process of changing the weights, and we say that the model is learning as it continues to train and the loss is reduced.

Categorical Cross-Entropy (CCE): One of the most often used cost/loss functions in classification. The goal is to reduce each class's entropy. The definition of CE for N classes is given below in equation 4.7:

$$\text{CE} = \frac{1}{M} \sum_{n=1}^{\infty} g_{0i} \log \text{p0i} \qquad 4.7$$

The above equation indicates that i is the foreground class, while p0i and g_{0i} stand for the projected probability of each class and the corresponding ground truth, respectively.

The idea of one-hot encoding is logically introduced with this notation. If there are M classes and you want to identify which class a sample belongs to, you create a binary vector that is only high for the class the sample belongs to. It is important to keep in mind that this is also an assumption regarding CE, as there are only hard memberships.

Sparse Cross-Entropy: When true labels are one-hot encoded, categorical cross-entropy is utilized. For instance, the true values for the three-class classification task are [1,0,0], [0,1,0], and [0,0,1]. Truth labels are integer encoded in sparse categorical cross-entropy, for instance, [1], [2], and [3] for a 3-class task.

4.2.8 Activation Function

The activation functions are yet another essential element of every neural network. The basic objective of these is to incorporate nonlinear modifications across layers, which could still allow a classifier to segregate nonlinearly separable data. A neural network cannot learn or represent more complex characteristics in the data without them. In terms of deep learning, this is crucial. By forcing output values to fall inside the range [0, 1], these functions may be used to convert data to a domain of interest and represent probability.

ReLU: The ReLU (Rectified Linear Unit) is the most often used activation function in deep learning models. This function may be shown in equation 4.8 as given below:

$$f(x) = \max(0, x) \qquad 4.8$$

where x = an input value

ReLu produces the highest value between zero and the input value, according to equation 1. When the input value is negative, the output is equal to zero, and when it is positive, it is equal to the input value. In light of this, equation 4.9 may be rewritten as follows:

$$f(x) = \begin{cases} 0, & x < 0 \\ x, & x \geq 0 \end{cases} \qquad 4.9$$

Where x = an input value

The function produces different results based on the inputs. For example, when x equals -6, the result of f (-6) is 0. In contrast, the result of f (0) is 0 because the input is higher or equal to 0. Furthermore, the outcome of f (6) is 5 because the input is larger than zero.

In order to get activation values for each neuron in neural networks, various common non-linear activation functions, such as sigmoid functions (or logistic) and hyperbolic tangent, are frequently utilized. To determine the activation levels in a conventional neural network or deep

neural network paradigms recently, the ReLu function has been applied. ReLu was chosen in place of the sigmoid and hyperbolic tangent for the following reasons:

1) **Simpler Computation:** The derivative remains constant, i.e. 1, given a positive input, reducing the time required for the model to train and minimizing mistakes.
2) **Representational Sparsity:** It has the ability to produce an actual value of zero.
3) **Linearity:** Smooth flow and easy optimization are two benefits of linear activation functions. Therefore, it works best for supervised tasks using big amounts of labeled data.

Softmax: In the last final layer, the activation function is often either a sigmoid or a softmax. The sigmoid function can only be applied when there are two classes only, but the softmax function may be applied with any number of classes. Softmax may be viewed as a particular instance of sigmoid, and as a result, softmax is typically the favored choice as long as the input is organized appropriately, i.e. utilizing one-hot encoding. Definition of softmax for k no. classes are given below equation 4.10:

$$\sigma(z)j = \frac{e^{zj}}{\sum_{k=1}^{k} e^{zk}}, \; j = 1,\ldots,k. \qquad 4.10$$

The multi-class logistic regression or softargmax function is another name for the softmax function. Softmax generalizes the logistic function by limiting values to [0, 1]. During the process of making a prediction based on an input, each category is given values that add up to 1. As a result, softmax may be used in the same way as a confidence predictor. The most likely category may be determined by extracting the category with the largest softmax result, which is the category in which the network has the most confidence that the sample belongs.

The results might be taken as a probability. However, it only bases its confidence on what it has observed during training, and at the output layer, it is compelled to make a prediction. Results should be viewed cautiously since their behavior cannot be predicted or controlled if an outlier

input that deviates from those seen during training is used. If one trained a cars/tucks classifier and fed it a train, it would still categorize the carrot as either a cars/ tucks. As a result, in the two-class situation, putting a threshold at 0.5 may not always be the optimal decision, because we cannot always interpret it as 50% probability.

Dropout: In the context of a neural network, the term "dropout" refers to the process of removing nodes from the input and hidden layers (as seen in Figure 4.7). As a result of the temporary removal of all connections going forward and backwards with a dropped node, a new network architecture might be created out of the parent network. A dropout probability of p causes the nodes to be removed from the graph.

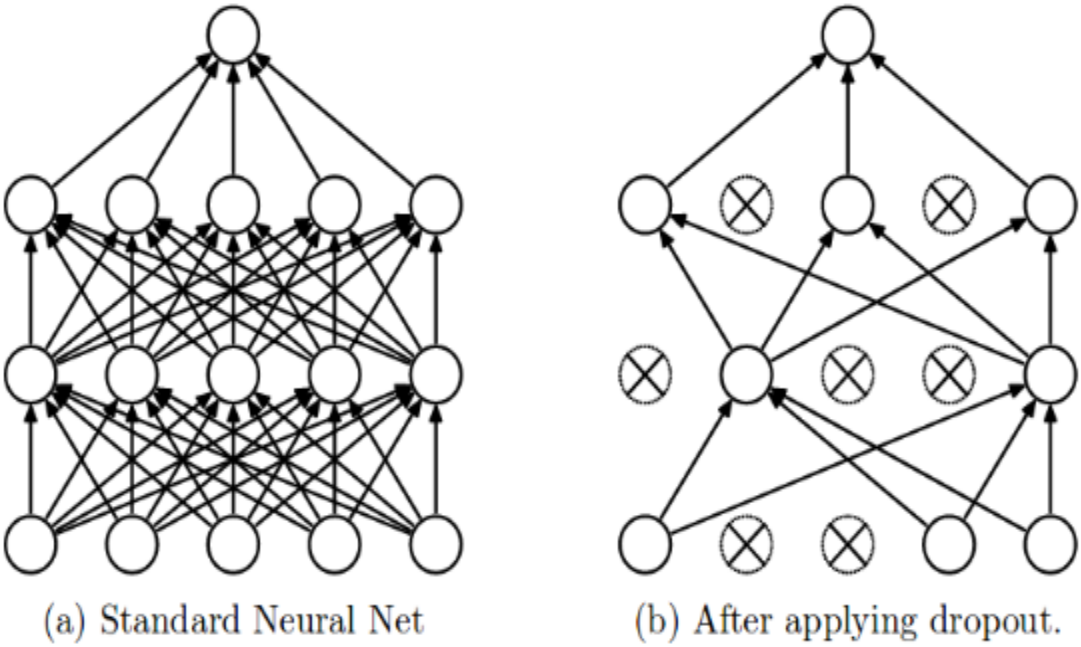

Figure 4.7 shows the Dropout operation being performed on a Standard Neural Network [67].

4.3 Experimental Setup

For this research work, I have used Google Colab as it provide 8GB of RAM and high speed computational power of GPU's. In this research work, I have used LIDC-IDRI dataset which contain high quality of images and to train model on such high resolution images we need high speed processing GPU. Python programming language has been used with necessary libraries like Tensor Flow, Seaborn, Keras, and Matplotlib. A table of experiment setup is given below in table 4.1.

Table 4.1: Experiment Setup

Development Environment	Google Colab
Hardware	Laptop DELL Inspiron Core i5-6200U, 8GB RAM DDR3-SDRAM, 500 GB HDD
Programming Language	Python 3.7.0
Libraries	Tensor Flow, Keras, Seaborn, Matplotlib
Evaluation Metric	Accuracy, Recall, F1 Score, Precision

As I mentioned above that I have used Google Colab for implementation of this research work. Firstly, I have set path and then load a dataset into Colab. When data is loaded successfully then I have import and install all necessary libraries and APIs. Then perform preprocessing, label conversion, and splitting of data into training and testing. To make dataset unbiased I have perform data augmentation on negative sample. Finally, we apply deep convolutional neural network model called VGG16 and train it on LIDC-IDRI database for both training and testing purpose. Furthermore, different evaluation metric as mention in table are used to check its performance score.

CHAPTER 5

RESULT DISCUSSION AND COMPARISON

5.1 Overview

This chapter presents the results and hyperparameters discussion and also present the comparison of the results of this study with other relevant studies in this domain. Hyperparameters significance to achieve the good results is also the part of this chapter.

5.2 Performance Metrics

To evaluate the performance of the proposed machine learning (ML) and deep learning (DL) techniques for detecting and classifying pulmonary nodules, various evaluation metric are used. In this study [68], the authors use Evaluation metrics including sensitivity (SE), specificity (SP), accuracy (ACC), precision (PPV), F1-score, Receiver Operating Characteristic (ROC) curve, Free Response Operating Characteristic (FROC) , Competition Performance Metric (CPM) and area under the ROC curve (AUC). Table 2.1 represents the evaluation metrics used in machine learning and deep neural networks for nodules detection and classification techniques

Table 5.1 Evaluation metrics used in ML and DNN for pulmonary nodule detection and classification

Evaluation Metrics	Definition
Sensitivity, TPR, Recall	$\mathrm{TPR} = \frac{\mathrm{TP}}{\mathrm{TP+FN}} = \frac{\mathrm{TP}}{\mathrm{P}}$
Specificity, TNR	$\mathrm{TNR} = \frac{\mathrm{TN}}{\mathrm{FP+TN}} = \frac{\mathrm{TN}}{\mathrm{N}}$
Accuracy	$\mathrm{Acccuracy} = \frac{\mathrm{TP+TN}}{\mathrm{TP+TN+FP+FN}}$
Precision	$\mathrm{PPV} = \frac{\mathrm{TP}}{\mathrm{TP+FN}}$
FPR	$\mathrm{FPR} = \frac{\mathrm{FP}}{\mathrm{FP+TN}}$
FNR	$\mathrm{FNR} = \frac{\mathrm{FN}}{\mathrm{TP+FN}}$
ROC	The graphical curve represent the relation among sensitivity or TPR on y-axis and specificity or FPR on x-axis
FROC	Similar to receiver operating characteristic graphical curve, just replace the FPR on X-axis with no. of false positives / image or scan.
LOGLOSS	Analyze the classifier's performance $$LogLoss = -\frac{1}{n}\sum_{i=1}^{n}[\ y_i \log(y_i) + \ (1 - y_i) \log(1 - y_i)]$$ 'n' for no. of patients in the test, yi for predicted cancer probability in patient (1 or 0).
CV	To analyze ML methods using a small dataset sample. CV reduce over-fitting and increase model generalization due to its frequent used in training phase of predicative models.

Note: T = True, F = False, N= Negative, R = Rate, ROC = Receiver Operating Characteristic, CV= Cross Validation

5.3 Result Discussion and Comparison

In this section, results of the study obtained after the implementation process have been discussed. I have already discussed the implementation methodology step by step, but in a concise and comprehensive way.

5.3.1 Result Discussion

I have already discussed that in this study VGG16 is used which is deep learning based convolutional neural network model and mainly used for the objects detection and classification problems. Moreover, a well-known dataset LIDC-IDRI is used here which contain the computed tomography (CT) scans of lung nodules or lung cancers. Here, fine-tuned VGG16 has been used with hyper-parameters tuning. Different evaluation matrices that have been used here are, Accuracy, Precision, Recall and F1-Score. Hyper-parameters that have been applied in this research work are given below in table 5.2.

Table 5.2: Summary of hyper parameters used in this research work

Batch Size	04
No. of Epochs	20
Loss	Sparse Categorical Cross Entropy
Dropout value	0.5
Activation Function	ReLU (Rectified Linear Unit)
Optimizer	Adam
Learning Rate	1e-4
Output Layer	Softmax

Results of the study in terms of accuracy and loss, achieved by the model are 0.9355 (93.55%) and 0.6853 respectively and both are indicate below in Figure 5.1 and Figure 5.2 respectively.

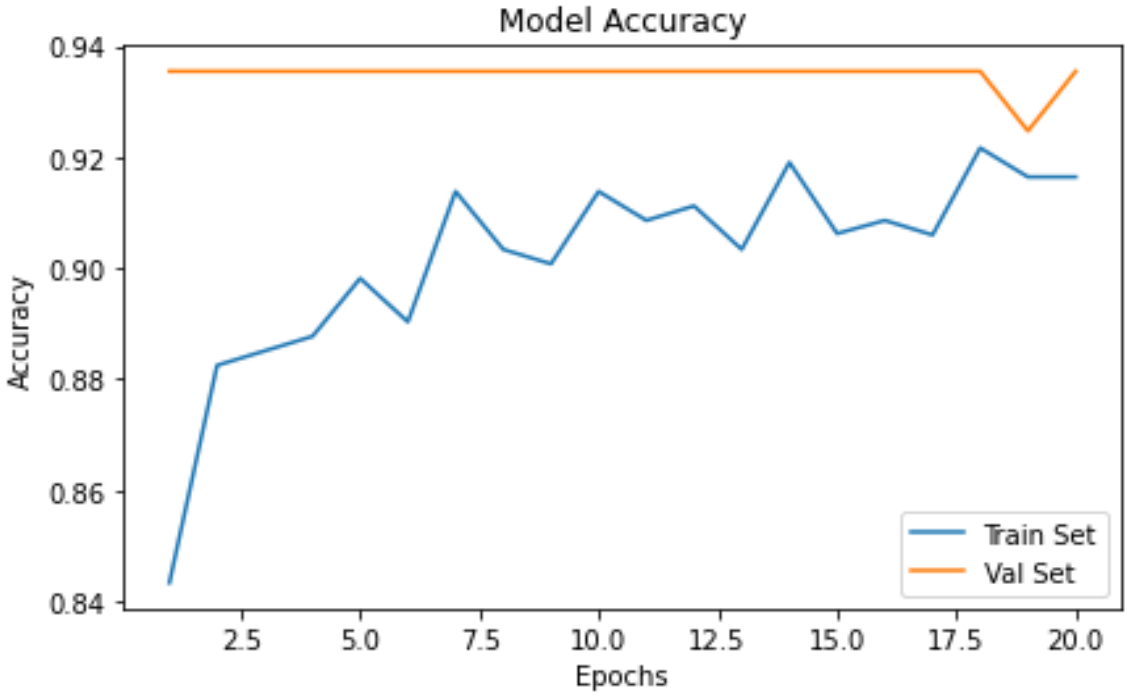

Figure 5.1: Model Accuracy

In the above given figure, accuracy of the model on train set is represented by blue line while the validation set accuracy is represented by an orange line. Horizontal axis is representing the number of epochs while vertical axis is showing the accuracy of the model on each epoch.

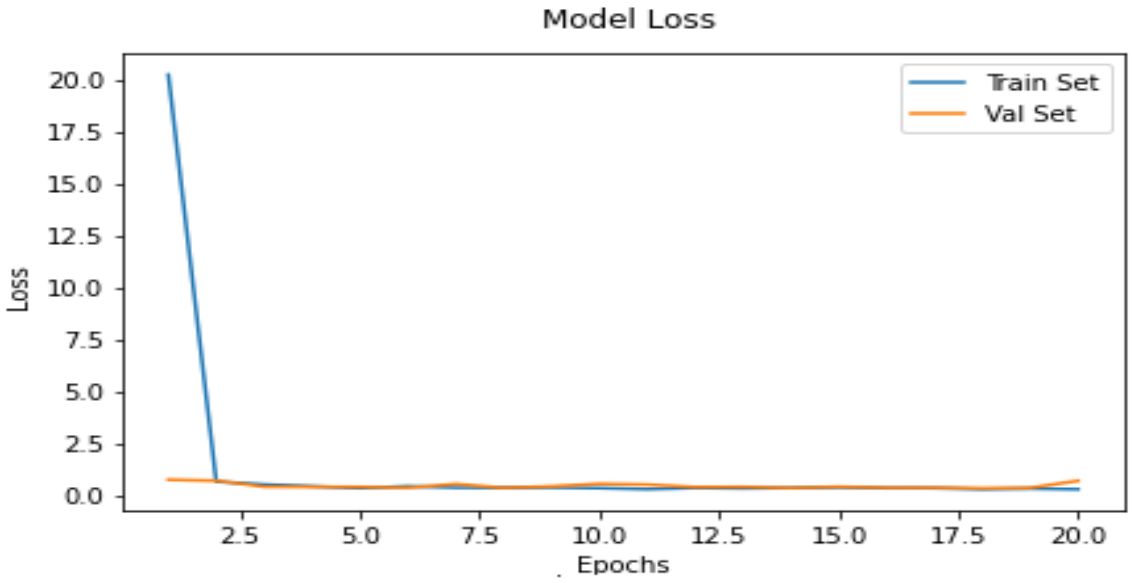

Figure 5.2: Model loss on each epoch

In the above given figure, loss score is being computed on the vertical axis while number of epochs are given on the horizontal axis. Blue line is representing the model loss on train set and orange line is representing the model loss on validation set which is also called as validation loss. Moreover, some other evaluation matrices have also been used here including Precision, recall and F1-Score and the results of them are given below respectively.

Table 5.3: Precision, Recall and F1-Score results with weighted average

Precision	0.8751 (87.51%)
Recall	0.9354 (93.54%)
F1-Score	0.9043 (90.43%)

These results have been achieved using weighted averages which is also shown below in Figure 5.3.

```
 Precision , Recall and F Score using Micro Average
(0.9354838709677419, 0.9354838709677419, 0.9354838709677419, None)
 Precision , Recall and F Score using weighted Average
(0.8751300728407907, 0.9354838709677419, 0.9043010752688171, None)
```

Figure 5. 3: Precision, Recall and F1-Score results using Micro Average and Weighted Average

Moreover, I have also used confusion matrix to further analyze the performance of my classification algorithm and also to calculate the false positive scores as it is one of the main objective of this research study to decrease the false positive score. A confusion matrix is usually used to calculate and visualize the values like true positive (TP), false negative (FN), false positive (FP) and true negative (TN). In Figure 5.4, it is clearly indicate that overall performance achieved by the suggested algorithm with respect to accuracy is 0.9355 percent while the false positive ratio is 0.0645 percent which is significantly low than previous studies in this domain.

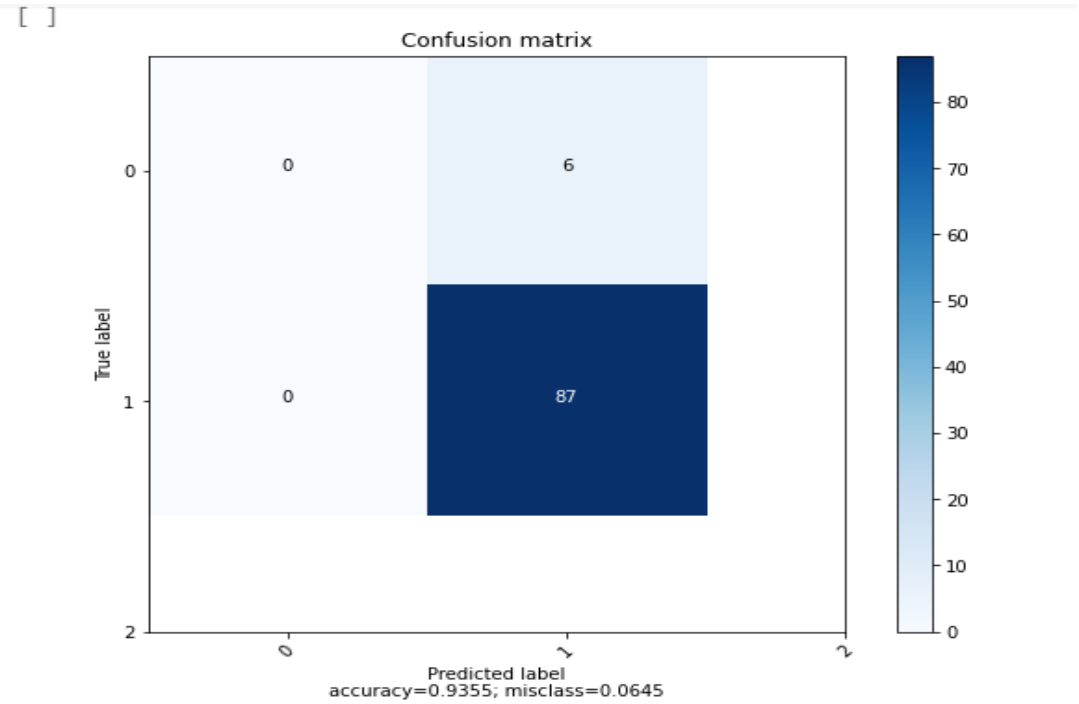

Figure 5.4: Confusion matrix

From the above given figure, it is evident that the main objectives of the study has been achieved. Accuracy has been significantly improved and false positive score has been reduced as well.

5.3.2 Results Comparison

In this research study, I have worked on the classification problem of lung nodules by considering all the size of nodules with an objective to attain the better accuracy with false positive reduction. Results achieved in this study in terms of accuracy, precision, recall and f1-score are 0.9355, 0.8751, 0.9354 and 0.9043 respectively. While false positive score is 0.0645 which is significantly low than previous studies. A comparison table of the results of this study with previous studies is given below in table.

Table 5.4: Result Comparison

Study	**Models**	**Accuracy**	**Precision**	**Recall**	**F1-Score**
Wu et al. [25]	DB U-Net	Not Given	Not given	88.51%	Not Given
Huang et al. [18]	3D CNN	Not given	Not Given	90%	Not Given
Xie et al. [21]	ResNet-50	91.60%	**87.75%**	86.52%	87.13%
My Approach	VGG-16	**93.55%**	87.51%	**93.54%**	**90.43%**

From the above table, it is evident that my approach outperformed the relate study in this domain and achieved a better joint accuracy as compared to the above mentioned study.

5.4 Summary

In this chapter, obtained results after the implementation work have been discussed. Moreover, all those parameters and hyper parameters that can significantly impact the results in a positive way have been discussed. These hyper parameters play a vital role to obtain the accurate and optimum results. Loss, accuracy, f1-score, precision, recall and false positive scores have been calculated in this study. Moreover, a comparison of the results with other most relevant studies in this domain is also the part of this chapter.

CHAPTER 6

CONCLUSION AND FUTURE WORK

6.1 Conclusion

To address the problem of candidate nodule detection and classification effectively using CT scan image, many researchers have used machine learning and computer vision-based techniques but these studies mostly do not consider the small size of lung nodules and ignore them. Moreover, these studies also suffer from the false-positive ratio which greatly affects the accuracy of the CAD system. In this study, I have developed Computer Aided Diagnostic (CAD) system for accurate detection and classification of lung candidate nodules of every size based on a deep learning network model VGG16. The suggested model VGG 16 achieve excellent results on both pulmonary nodule identification and malignancy classification problems on the publicly accessible LIDC-IDRC dataset. This technique involved the steps of lung nodules image data acquisition, preprocessing of the images, data augmentation, and feature extraction using a deep convolutional neural network (DCNN). Then DCNN model is trained and classification of nodules has been performed into cancerous and non-cancerous. This research work is tested and evaluated on LIDC-IDRI openly available dataset. The experimental work shows that the DCNN model VGG 16 achieved excellent performance with an accuracy of 93.55%, recall of 93.54%, and precision of 87.15% respectively which is better than the results gained by a previous study in this domain 91.60%.

This research study has also some limitation which will be handle in near future. First, there is still a space available to reduce the score of false nodules. Secondly, data available for nodule detection and classification is not enough, so in future I will evaluate my developed system on more dataset which are publicly available and even create my own private database for better accuracy and sensitivity.

6.2 Future work

Computer aided diagnosis systems are playing an important role in various domains of the healthcare sector and no one can deny the importance of such systems. Lungs cancer is one of the leading type of cancer in the world that has more mortality rate. One of the main reason of this mortality rate is the late diagnosis or misdiagnosis of the lung cancer and misclassification of the nodules due to the varying size of nodules. Early detection, classification and avoiding the misclassification can significantly reduce this mortality rate. Deep learning is one of the field which has provided us some breakthroughs in this domain. In this research work, I have focused on the accurate and improved classification accuracy with significantly reduced misclassification and obtained very promising words. In future, by combining all the authentic datasets that are available related to this domain and by applying other techniques such as GANs (Generative adversarial networks) and more deep learning models can help us to achieve better results and false positive ratio can be reduced further hence improving the accurate classification within fewer minutes

References

[1] NIH, “What Is Cancer ? Differences between Cancer Cells and Normal Cells,” *Natl. Cancer Inst.*, pp. 1–8, 2021, [Online]. Available: https://www.cancer.gov/about-cancer/understanding/what-is-cancer.

[2] C. Agencies, “Cancer,” vol. 2020, no. March, pp. 1–7, 2020, [Online]. Available: https://www.who.int/news-room/fact-sheets/detail/cancer.

[3] H. Sung *et al.*, “Global Cancer Statistics 2020: GLOBOCAN Estimates of Incidence and Mortality Worldwide for 36 Cancers in 185 Countries,” *CA. Cancer J. Clin.*, vol. 71, no. 3, pp. 209–249, 2021, doi: 10.3322/caac.21660.

[4] “Key Statistics for Lung Cancer,” *Am. Cancer Soc.*, vol. 5, no. January, 2020, [Online]. Available: https://www.cancer.org/cancer/lung-cancer/about/key-statistics.html.

[5] C. S. Dela Cruz, L. T. Tanoue, and R. A. Matthay, “Lung Cancer: Epidemiology, Etiology, and Prevention,” *Clin. Chest Med.*, vol. 32, no. 4, pp. 605–644, 2011, doi: 10.1016/j.ccm.2011.09.001.

[6] H. Zeng *et al.*, “Cancer survival in China, 2003-2005: A population-based study,” *Int. J. Cancer*, vol. 136, no. 8, pp. 1921–1930, 2015, doi: 10.1002/ijc.29227.

[7] N. Camarlinghi, “Automatic detection of lung nodules in computed tomography images: training and validation of algorithms using public research databases,” *Eur. Phys. J. Plus*, vol. 128, no. 9, 2013, doi: 10.1140/epjp/i2013-13110-5.

[8] W. J. Kostis, A. P. Reeves, D. F. Yankelevitz, and C. I. Henschke, “Three-Dimensional Segmentation and Growth-Rate Estimation of Small Pulmonary Nodules in Helical CT Images,” *IEEE Trans. Med. Imaging*, vol. 22, no. 10, pp. 1259–1274, 2003, doi: 10.1109/TMI.2003.817785.

[9] H. Macmahon *et al.*, “Guidelines for Management of Incidental Pulmonary Nodules Detected on CT Images,” *Radiol. n Radiol.*, vol. 000, no. 284, pp. 228–243, 2017, [Online]. Available: http://pubs.rsna.org/doi/pdf/10.1148/radiol.2017161659.

[10] S. G. Armato *et al.*, “The Lung Image Database Consortium (LIDC) and Image Database Resource Initiative (IDRI): A completed reference database of lung nodules on CT scans,”

Med. Phys., vol. 38, no. 2, pp. 915–931, 2011, doi: 10.1118/1.3528204.

[11] N. Bhaskar and T. S. Ganashree, "A Model : Lung Nodule Detection and Classification by SVM Network," *Eur. J. Mol. Clin. Med.*, vol. 7, no. 8, pp. 3228–3238, 2020.

[12] O. Ozdemir, R. L. Russell, and A. A. Berlin, "A 3D Probabilistic Deep Learning System for Detection and Diagnosis of Lung Cancer Using Low-Dose CT Scans," *IEEE Trans. Med. Imaging*, vol. 39, no. 5, pp. 1419–1429, 2020, doi: 10.1109/TMI.2019.2947595.

[13] A. Sheeraz, J. M. Younus, A. M. Usman, Q. Usman, and H. Ali, "Pulmonary nodules detection and classification using hybrid features from computerized tomographic images," *J. Med. Imaging Heal. Informatics*, vol. 6, no. 1, pp. 252–259, 2016, doi: 10.1166/jmihi.2016.1600.

[14] K. Senthil Kumar, K. Venkatalakshmi, and K. Karthikeyan, "Lung Cancer Detection Using Image Segmentation by means of Various Evolutionary Algorithms," *Comput. Math. Methods Med.*, vol. 2019, 2019, doi: 10.1155/2019/4909846.

[15] X. Y. Jin, Y. C. Zhang, and Q. L. Jin, "Pulmonary Nodule Detection Based on CT Images Using Convolution Neural Network," *Proc. - 2016 9th Int. Symp. Comput. Intell. Des. Isc. 2016*, vol. 1, pp. 202–204, 2016, doi: 10.1109/ISCID.2016.1053.

[16] C. Wang, A. Elazab, J. Wu, and Q. Hu, "Lung nodule classification using deep feature fusion in chest radiography," *Comput. Med. Imaging Graph.*, vol. 57, pp. 10–18, 2017, doi: 10.1016/j.compmedimag.2016.11.004.

[17] N. Tajbakhsh and K. Suzuki, "Comparing two classes of end-to-end machine-learning models in lung nodule detection and classification: MTANNs vs. CNNs," *Pattern Recognit.*, vol. 63, pp. 476–486, 2017, doi: 10.1016/j.patcog.2016.09.029.

[18] X. Huang, J. Shan, and V. Vaidya, "Lung nodule detection in CT using 3D convolutional neural networks," *Proc. - Int. Symp. Biomed. Imaging*, pp. 379–383, 2017, doi: 10.1109/ISBI.2017.7950542.

[19] J. Ding, A. Li, Z. Hu, and L. Wang, "Accurate pulmonary nodule detection in computed tomography images using deep convolutional neural networks," *Lect. Notes Comput. Sci. (including Subser. Lect. Notes Artif. Intell. Lect. Notes Bioinformatics)*, vol. 10435 LNCS, pp. 559–567, 2017, doi: 10.1007/978-3-319-66179-7_64.

[20] Q. Dou, H. Chen, L. Yu, J. Qin, and P. A. Heng, “Multilevel Contextual 3-D CNNs for False Positive Reduction in Pulmonary Nodule Detection,” *IEEE Trans. Biomed. Eng.*, vol. 64, no. 7, pp. 1558–1567, 2017, doi: 10.1109/TBME.2016.2613502.

[21] Y. Xie *et al.*, “Knowledge-based Collaborative Deep Learning for Benign-Malignant Lung Nodule Classification on Chest CT,” *IEEE Trans. Med. Imaging*, vol. 38, no. 4, pp. 991–1004, 2019, doi: 10.1109/TMI.2018.2876510.

[22] P. Monkam *et al.*, “Ensemble Learning of Multiple-View 3D-CNNs Model for Micro-Nodules Identification in CT Images,” *IEEE Access*, vol. 7, pp. 5564–5576, 2019, doi: 10.1109/ACCESS.2018.2889350.

[23] C. F. J. Kuo *et al.*, “Automatic lung nodule detection system using image processing techniques in computed tomography,” *Biomed. Signal Process. Control*, vol. 56, p. 101659, 2020, doi: 10.1016/j.bspc.2019.101659.

[24] A. AbuBaker and Y. Ghadi, “A novel CAD system to automatically detect cancerous lung nodules using wavelet transform and SVM,” *Int. J. Electr. Comput. Eng.*, vol. 10, no. 5, pp. 4745–4751, 2020, doi: 10.11591/ijece.v10i5.pp4745-4751.

[25] Z. Wu, Q. Zhou, and F. Wang, “Coarse-to-Fine Lung Nodule Segmentation in CT Images with Image Enhancement and Dual-Branch Network,” *IEEE Access*, vol. 9, pp. 7255–7262, 2021, doi: 10.1109/ACCESS.2021.3049379.

[26] H. Cao *et al.*, “A Two-Stage Convolutional Neural Networks for Lung Nodule Detection,” *IEEE J. Biomed. Heal. Informatics*, vol. 24, no. 7, pp. 2006–2015, 2020, doi: 10.1109/JBHI.2019.2963720.

[27] A. Soliman *et al.*, “Accurate lungs segmentation on CT chest images by adaptive appearance-guided shape modeling,” *IEEE Trans. Med. Imaging*, vol. 36, no. 1, pp. 263–276, 2017, doi: 10.1109/TMI.2016.2606370.

[28] G. Aresta *et al.*, “iW-Net: an automatic and minimalistic interactive lung nodule segmentation deep network,” *Sci. Rep.*, vol. 9, no. 1, pp. 1–9, 2019, doi: 10.1038/s41598-019-48004-8.

[29] T. Nemoto *et al.*, “Efficacy evaluation of 2D, 3D U-Net semantic segmentation and atlas-based segmentation of normal lungs excluding the trachea and main bronchi,” *J. Radiat.*

Res., vol. 61, no. 2, pp. 257–264, 2020, doi: 10.1093/jrr/rrz086.

[30] T. Zhao, D. Gao, J. Wang, and Z. Tin, "Lung segmentation in CT images using a fully convolutional neural network with multi-instance and conditional adversary loss," *Proc. - Int. Symp. Biomed. Imaging*, vol. 2018-April, no. Isbi, pp. 505–509, 2018, doi: 10.1109/ISBI.2018.8363626.

[31] Z. Xiao, B. Liu, L. Geng, F. Zhang, and Y. Liu, "Segmentation of lung nodules using improved 3D-UNet neural network," *Symmetry (Basel).*, vol. 12, no. 11, pp. 1–15, 2020, doi: 10.3390/sym12111787.

[32] H. Shaziya, K. Shyamala, and R. Zaheer, "Automatic Lung Segmentation on Thoracic CT Scans Using U-Net Convolutional Network," *Proc. 2018 IEEE Int. Conf. Commun. Signal Process. ICCSP 2018*, pp. 643–647, 2018, doi: 10.1109/ICCSP.2018.8524484.

[33] M. Z. Alom, C. Yakopcic, M. Hasan, T. M. Taha, and V. K. Asari, "Recurrent residual U-Net for medical image segmentation," *J. Med. Imaging*, vol. 6, no. 01, p. 1, 2019, doi: 10.1117/1.jmi.6.1.014006.

[34] N. V. Keetha, S. A. B. P, and C. S. R. Annavarapu, "U-Det: A Modified U-Net architecture with bidirectional feature network for lung nodule segmentation," pp. 1–14, 2020, [Online]. Available: http://arxiv.org/abs/2003.09293.

[35] B. N. Narayanan, R. C. Hardie, T. M. Kebede, and M. J. Sprague, "Optimized feature selection-based clustering approach for computer-aided detection of lung nodules in different modalities," *Pattern Anal. Appl.*, vol. 22, no. 2, pp. 559–571, 2019, doi: 10.1007/s10044-017-0653-4.

[36] G. Aresta, A. Cunha, and A. Campilho, "Detection of juxta-pleural lung nodules in computed tomography images," *Med. Imaging 2017 Comput. Diagnosis*, vol. 10134, no. March 2017, p. 101343N, 2017, doi: 10.1117/12.2252022.

[37] S. A. Mehre, S. Mukhopadhyay, A. Dutta, N. C. Harsha, A. K. Dhara, and N. Khandelwal, "An automated lung nodule detection system for CT images using synthetic minority oversampling," *Med. Imaging 2016 Comput. Diagnosis*, vol. 9785, no. March 2016, p. 97850H, 2016, doi: 10.1117/12.2216357.

[38] D. Cascio, R. Magro, F. Fauci, M. Iacomi, and G. Raso, "Automatic detection of lung

nodules in CT datasets based on stable 3D mass-spring models," *Comput. Biol. Med.*, vol. 42, no. 11, pp. 1098–1109, 2012, doi: 10.1016/j.compbiomed.2012.09.002.

[39] A. El-Baz, A. Elnakib, M. Abou El-Ghar, G. Gimel'Farb, R. Falk, and A. Farag, "Automatic detection of 2D and 3D lung nodules in chest spiral CT scans," *Int. J. Biomed. Imaging*, vol. 2013, 2013, doi: 10.1155/2013/517632.

[40] Mohammad, S. T. Gity, MasoumehNamin, H. A. Moghaddam, R. Jafari, and Esmaeil-Zadeh, "Automated detection and classification of pulmonary nodules in 3D thoracic CT images," *Conf. Proc. - IEEE Int. Conf. Syst. Man Cybern.*, pp. 3774–3779, 2010, doi: 10.1109/ICSMC.2010.5641820.

[41] H. Jiang, H. Ma, W. Qian, M. Gao, and Y. Li, "An Automatic Detection System of Lung Nodule Based on Multigroup Patch-Based Deep Learning Network," *IEEE J. Biomed. Heal. Informatics*, vol. 22, no. 4, pp. 1227–1237, 2018, doi: 10.1109/JBHI.2017.2725903.

[42] S. Zheng, J. Guo, X. Cui, R. N. J. Veldhuis, M. Oudkerk, and P. M. A. Van Ooijen, "Automatic Pulmonary Nodule Detection in CT Scans Using Convolutional Neural Networks Based on Maximum Intensity Projection," *IEEE Trans. Med. Imaging*, vol. 39, no. 3, pp. 797–805, 2020, doi: 10.1109/TMI.2019.2935553.

[43] H. Cheng, Y. Zhu, and H. Pan, "Modified U-Net block network for lung nodule detection," *Proc. 2019 IEEE 8th Jt. Int. Inf. Technol. Artif. Intell. Conf. ITAIC 2019*, no. Itaic, pp. 599–605, 2019, doi: 10.1109/ITAIC.2019.8785445.

[44] H. Hu, Q. Li, Y. Zhao, and Y. Zhang, "Parallel Deep Learning Algorithms with Hybrid Attention Mechanism for Image Segmentation of Lung Tumors," *IEEE Trans. Ind. Informatics*, vol. 17, no. 4, pp. 2880–2889, 2021, doi: 10.1109/TII.2020.3022912.

[45] X. Huang, W. Sun, T. L. (Bill) Tseng, C. Li, and W. Qian, "Fast and fully-automated detection and segmentation of pulmonary nodules in thoracic CT scans using deep convolutional neural networks," *Comput. Med. Imaging Graph.*, vol. 74, pp. 25–36, 2019, doi: 10.1016/j.compmedimag.2019.02.003.

[46] J. J. Suárez-Cuenca, W. Guo, and Q. Li, "Automated detection of pulmonary nodules in CT: false positive reduction by combining multiple classifiers," *Med. Imaging 2011 Comput. Diagnosis*, vol. 7963, no. March 2011, p. 796338, 2011, doi: 10.1117/12.878793.

[47] S. A. El-Regaily, M. A. M. Salem, M. H. Abdel Aziz, and M. I. Roushdy, "Multi-view Convolutional Neural Network for lung nodule false positive reduction," *Expert Syst. Appl.*, vol. 162, p. 113017, 2020, doi: 10.1016/j.eswa.2019.113017.

[48] T. S. Roy, N. Sirohi, and A. Patle, "Classification of lung image and nodule detection using fuzzy inference system," *Int. Conf. Comput. Commun. Autom. ICCCA 2015*, pp. 1204–1207, 2015, doi: 10.1109/CCAA.2015.7148560.

[49] V. Mekali and H. Girijamma, "Fully automatic detection and segmentation approach for juxta-pleural nodules from ct images," *Int. J. Healthc. Inf. Syst. Informatics*, vol. 16, no. 2, pp. 87–104, 2021, doi: 10.4018/IJHISI.20210401.oa5.

[50] A. Halder, S. Chatterjee, and D. Dey, "Morphological Filter Aided GMM Technique for Lung Nodule Detection," *Proc. 2020 IEEE Appl. Signal Process. Conf. ASPCON 2020*, pp. 198–202, 2020, doi: 10.1109/ASPCON49795.2020.9276715.

[51] S. M. Naqi, M. Sharif, and A. Jaffar, "Lung nodule detection and classification based on geometric fit in parametric form and deep learning," *Neural Comput. Appl.*, vol. 32, no. 9, pp. 4629–4647, 2020, doi: 10.1007/s00521-018-3773-x.

[52] E. Rendon-Gonzalez and V. Ponomaryov, "Automatic Lung nodule segmentation and classification in CT images based on SVM," *9th Int. Kharkiv Symp. Phys. Eng. Microwaves, Millim. Submillim. Waves, MSMW 2016*, no. June, pp. 1–4, 2016, doi: 10.1109/MSMW.2016.7537995.

[53] Y. Gu *et al.*, "Automatic lung nodule detection using a 3D deep convolutional neural network combined with a multi-scale prediction strategy in chest CTs," *Comput. Biol. Med.*, vol. 103, pp. 220–231, 2018, doi: 10.1016/j.compbiomed.2018.10.011.

[54] P. M. Bruntha *et al.*, "Lung Nodule Classification using Shallow CNNs and Deep Transfer Learning CNNs," *2021 7th Int. Conf. Adv. Comput. Commun. Syst. ICACCS 2021*, pp. 1474–1478, 2021, doi: 10.1109/ICACCS51430.2021.9441702.

[55] S. M. Naqi, M. Sharif, and I. U. Lali, "A 3D nodule candidate detection method supported by hybrid features to reduce false positives in lung nodule detection," *Multimed. Tools Appl.*, vol. 78, no. 18, pp. 26287–26311, 2019, doi: 10.1007/s11042-019-07819-3.

[56] R. Manickavasagam and S. Selvan, "Automatic Detection and Classification of Lung

Nodules in CT Image Using Optimized Neuro Fuzzy Classifier with Cuckoo Search Algorithm," *J. Med. Syst.*, vol. 43, no. 3, 2019, doi: 10.1007/s10916-019-1177-9.

[57] P. Kavitha and S. Prabakaran, "A novel hybrid segmentation method with particle swarm optimization and fuzzy c-mean based on partitioning the image for detecting lung cancer," *Int. J. Eng. Adv. Technol.*, vol. 8, no. 5, pp. 1223–1227, 2019, doi: 10.20944/preprints201906.0195.v1.

[58] F. Liao, M. Liang, Z. Li, X. Hu, and S. Song, "Evaluate the Malignancy of Pulmonary Nodules Using the 3-D Deep Leaky Noisy-OR Network," *IEEE Trans. Neural Networks Learn. Syst.*, vol. 30, no. 11, pp. 3484–3495, 2019, doi: 10.1109/TNNLS.2019.2892409.

[59] K. Parrish, "Deep Learning vs. Machine Learning: What's the difference between two?," *Digitaltrends*, pp. 1–9, 2018, [Online]. Available: https://www.digitaltrends.com/cool-tech/deep-learning-vs-machine-learning-explained/.

[60] Anne Bonner, "What is Deep Learning and How Does it Work?," *Towar. Data Sci.*, pp. 1–10, 2019.

[61] A. Lenail, "NN-SVG : Publication-Ready Neural Network Architecture Schematics," vol. 4, no. 1998, p. 21105, 2019, doi: 10.21105/joss.00747.

[62] L. Posts, "Backpropagation Neural Network using Python What is Backpropagation Neural Network (BPN)?," pp. 1–13, 2022.

[63] S. Ruder, "An overview of gradient descent optimization algorithms," pp. 1–14, 2016, [Online]. Available: http://arxiv.org/abs/1609.04747.

[64] S. Theodoridis and K. Koutroumbas, *Pattern Recognition - minder good*. 2009.

[65] V. Bushaev, "Adam deep learning optimization," *Https://Towardsdatascience.Com/Adam-Latest-Trends-in-Deep-Learning-Optimization-6Be9a291375C*, pp. 1–18, 2018, [Online]. Available: https://towardsdatascience.com/adam-latest-trends-in-deep-learning-optimization-6be9a291375c.

[66] K. E. Koech, "Cross-Entropy Loss Function," pp. 1–8, 2020.

[67] N. Srivastava, G. Hinton, A. Krizhevsky, I. Sutskever, and R. Salakhutdinov, "Dropout: A simple way to prevent neural networks from overfitting," *J. Mach. Learn. Res.*, vol. 15,

pp. 1929–1958, 2014.

[68] D. M. W. Powers, “Evaluation: from precision, recall and F-measure to ROC, informedness, markedness and correlation,” pp. 37–63, 2020, [Online]. Available: http://arxiv.org/abs/2010.16061.